

5. SITE 578¹

Shipboard Scientific Party, with a contribution by Patricia Doyle²

HOLE 578

Date occupied: 27 May 1982

Date departed: 30 May 1982

Time on hole: 2 days, 6½ hr.

Position (latitude; longitude): 33°55.56'N; 151°37.74'E

Water depth (sea level; corrected m, echo-sounding): 6010

Water depth (rig floor; corrected m, echo-sounding): 6020

Bottom felt (m, drill pipe): 6005

Penetration (m): 176.8

Number of cores: 20

Total length of cored section (m): 167.8

Total core recovered (m): 165.02

Core recovery (%): 98

Oldest sediment cored:

Depth sub-bottom (m): 176.6

Nature: Chert and silicified chalk

Age: Campanian to Maestrichtian

Measured velocity (km/s): 1.52 (clay immediately above chert)

Basement: Not reached

Principal results: Hole 578 recovered a thick section of late Neogene siliceous clays. Siliceous microfossils are well represented in the late Quaternary and late Miocene-Pliocene portion of the section. The paleomagnetic stratigraphy is exceptionally good. All major events back to the middle of Epoch 5 can be identified even from the shipboard natural remanent magnetization (NRM) inclinations.

The upper 76.6 m of clay and siliceous clay (0–2.4 m.y. ago) is anoxic (gray and olive gray in color) with many pyrite-cemented layers. From 76.6 to 124.5 m (2.4 to 9–9.5 m.y. ago), the clays are oxidized (yellow brown and brown in color) with rare ferromanganese nodules. These two units contain 72 clearly visible ash layers, 24 of which are more than 5 cm thick (the thickest is 17 or 27 cm if adjoining 17 and 10 cm white and green ash beds formed from a single eruption).

From 124.5 to 176 m (9–9.5 to about 70 m.y. ago), the pelagic clay is "slick," predominantly dark to very dark brown, and very homogeneous. At its base, the clay is very stiff, with a shear strength approaching 2 kg/cm² (the 9.5 m core at a depth of 170 m penetrated only a little over 4 m). Drilling was stopped by chert at 176.8 m. Silicified foraminifers immediately above the chert are late Campanian to Maestrichtian in age (about 70 m.y.).

Sedimentation rates drop from almost 40 m/m.y. at the surface to about 25 m/m.y. from 1 to 2.4 m.y. ago, where they decrease abruptly to 15 m/m.y. and then gradually to about 8 m/m.y. at the base of the fossiliferous section. If deposition was continuous, the pelagic clays accumulated at less than 1 m/m.y. from about 10 to 70 m.y. ago. The rapid late Pliocene-Pleistocene sedimentation rates were unexpected. Further work is required to determine whether a change in provenance or transport was responsible for the 70% rate increase 2.4 m.y. ago.

BACKGROUND AND OBJECTIVES

Site 578 (target site NW-8A) lies at the join of the east-west and north-south traverses that make up most of Leg 86. On the east-west traverse, the site complements Site 576 because of its proximity to the Asian source of eolian debris and to the western boundary current of the North Pacific. For most of the Cenozoic, the pelagic clay section at Site 578 complements those at Site 576 and LL44-GPC3 to define the history of authigenic sedimentation in this large region.

On the north-south traverse, Site 578 provides the most subtropical paleoceanographic end member. The abrupt thickening of the "transparent" acoustic layer immediately to the south of the site may mark the southern limit of the Kuroshio return flow—the extreme southern limit of transition water in this area.

Our specific scientific objectives at Site 578 were

1. To obtain a detailed paleoceanographic record of the northern edge of the subtropical water mass for the late Cenozoic.

2. To determine the time of onset of significant bio-siliceous accumulation.

3. To interrelate tephrochronology, paleomagnetic stratigraphy, and biostratigraphy for a northwest Pacific late Cenozoic subtropical section.

4. To assess the nature and history of authigenic sedimentation during the late Cretaceous and Paleogene.

5. To determine the late Cretaceous and Cenozoic history of eolian sedimentation for comparison with the more distal Site 576 and LL44-GPC3.

6. To assess the nature of the red clay-chert boundary, particularly in terms of enhanced diagenesis of the basal clay.

Geologic and Topographic Setting

The regional seafloor morphology and echo character of the near-surface sediments of the northwest Pacific have been mapped by Damuth et al. (1983), using all

¹ Heath, G. R., Burckle, L. H., et al., *Init. Repts. DSDP*, 86: Washington (U.S. Govt. Printing Office).

² Addresses: (Shipboard Scientific Party) G. Ross Heath (Co-Chief Scientist) School of Oceanography, Oregon State University, Corvallis OR 97331 (present address: College of Ocean and Fishery Sciences, University of Washington, Seattle, WA 98195); Lloyd H. Burckle (Co-Chief Scientist) Lamont-Doherty Geological Observatory, Palisades, NY 10964; Anthony E. D'Agostino, ARCO Exploration Company, Houston, TX 77056; Ulrich Bleil, Institut für Geophysik, Ruhr-Universität Bochum, D-4630 Bochum Querenburg, Federal Republic of Germany; Ki-iti Horai, Lamont-Doherty Geological Observatory, Palisades, NY 10964 (present address: Meteorological College, Chiba University, Chiba 277, Japan); Robert D. Jacobi, Department of Geological Sciences, SUNY Buffalo, Amherst, NY 14226; Tom Janacek, Department of Atmospheric & Oceanic Science, University of Michigan, Ann Arbor, MI 48109 (present address: Lamont-Doherty Geological Observatory, Palisades, NY 10964); Itaru Koizumi, College of General Education, Osaka University, Osaka 560, Japan; Lawrence A. Krissiek, School of Oceanography, Oregon State University, Corvallis, OR 97331 (present address: Department of Geology and Mineralogy, Ohio State University, Columbus, OH 43210); Nicole Lenôtre, Bureau de Recherches Géologiques et Minières, Centre Océanologique de Bretagne, 45060 Orléans Cedex, France; Simonetta Monechi, Geological Research Division, Scripps Institution of Oceanography, La Jolla, CA 92093 (present address: Dipartimento di Scienze della Terra, Università di Firenze, 4 Via La Pira, 50121 Firenze, Italy); Joseph J. Morley, Lamont-Doherty Geological Observatory, Palisades, NY 10964; Peter Schultheiss, Institute of Oceanographic Sciences, Surrey GU8 5UB, United Kingdom; Audrey A. Wright, Deep Sea Drilling Project, Scripps Institution of Oceanography, La Jolla, CA 92093 (present address: Ocean Drilling Program, 500 University Drive West, Texas A&M University, College Station, TX 77843); (Doyle) Geological Research Division, Scripps Institution of Oceanography, La Jolla, CA 92093.

available Lamont-Doherty, Scripps, and Hawaii Institute of Geophysics 3.5-kHz reflection records. Site 578 lies west of Shatsky Rise in a large area of gently rolling sea-floor underlain by a section of continuous parallel sub-bottom reflectors up to several hundred meters thick above Cretaceous chert and chalk.

The area around Site 578 was surveyed in detail on R/V *Vema* Cruise 36-12. Based on the piston cores and 3.5-kHz records from the survey, a drill site was selected at 33°56'N, 151°38'E, a location typical of the north-western quadrant of the area. The topography is very subdued, with local relief of tens of meters over distances of tens of kilometers. The air gun 100-Hz reflection profiles show about 160 m of layered sediment above chert(?). From the V-36 piston cores, we suspected that a significant number of the laterally continuous shallow reflectors were ash beds.

The site lies in the magnetic bight, possibly on Anomaly M21. If so, the basement age is about 145 m.y.

OPERATIONS

From Site 577 we steamed east, across the west side of Shatsky Rise for 1½ days to Site 578 (target Site NW-8A). The air-gun, 3.5-, and 12-kHz records collected under way are of excellent quality.

The vessel entered the B-1 survey area of R/V *Vema* Cruise 36-12 on 26 May 1982(Z). The site was selected some 19 miles west-northwest of the original target Site NW-8A because shipboard assessment of the V-36 air-gun records indicated slightly more lateral uniformity at the alternate site. Because of the detail of the *Vema* survey and the acoustic uniformity of the upper part of the sediment section, the *Challenger* steamed directly to the site, dropped the beacon at 1900Z, and immediately retrieved the magnetometer and seismic gear.

Drill pipe run-in began at 2015Z on 26 May, with the first successful 9.5-m hydraulic piston corer (HPC) core on deck at 1326Z on 27 May. Despite good returns from both the ship's 3.5-kHz transducer and a 3.5-kHz pinger attached 251 m above the bit, the first core contained only water. We are unable to account for the large discrepancy (18% in the case of the pinger) between the acoustic and drill pipe depths. The location of the pinger on the string was rechecked on retrieval and found to be correct.

Coring proceeded without mishap for 20 cores (Table 1). Cores 17 to 20 did not stroke out completely due to the stiffness of the red clay below 150 m. We washed down 9.5 m between cores 17 to 20 to conserve time.

The overall quality of the HPC cores at this site was substantially better than the quality of those at Sites 576 and 577. We attribute this to the addition of an extra shear pin to the HPC which allowed it to fully pressure up before firing. We suspect that the intermittent flow-in seen in cores from the earlier sites resulted from premature shear pin failure followed by slow penetration of the HPC, which allowed the heave of the ship to move the piston as the core was being taken. Mike Storms' efforts to solve this problem are greatly appreciated.

The core nose heat-flow unit worked well, with seven successful deployments out of eight.

Table 1. Site 578 coring summary.

Core	Date (May 1982)	Local time	Depth from drill floor (m)	Depth below seafloor (m)	Length cored (m)	Length recovered (m)	Percent recovered
1	28	0226	6004.7-6009.5	0.0-4.8	4.8	4.77	99
2	28	0451	6009.5-6019.0	4.8-14.3	9.5	8.25	87
3	28	0707	6019.0-6028.5	14.3-23.8	9.5	9.70	102
4	28	0925	6028.5-6038.0	23.8-33.3	9.5	9.01	95
5	28	1150	6038.0-6047.5	33.3-42.8	9.5	9.63	101
6	28	1412	6047.5-6057.0	42.8-52.3	9.5	10.00	105
7	28	1640	6057.0-6066.5	52.3-61.8	9.5	9.68	102
8	28	1905	6066.5-6076.0	61.8-71.3	9.5	9.76	103
9	28	2132	6076.0-6085.5	71.3-80.8	9.5	9.75	103
10	29	0003	6085.5-6095.0	80.8-90.3	9.5	8.93	94
11	29	0231	6095.0-6104.5	90.3-99.8	9.5	9.44	99
12	29	0453	6104.5-6114.0	99.8-109.3	9.5	9.06	95
13	29	0725	6114.0-6123.5	109.3-118.8	9.5	9.48	100
14	29	0940	6123.5-6133.0	118.8-128.3	9.5	10.18	107
15	29	1204	6133.0-6142.5	128.3-137.8	9.5	9.76	103
16	29	1420	6142.5-6152.0	137.8-147.3	9.5	8.36	88
17	29	1642	6152.0-6160.0	147.3-155.3	8.0	7.68	96
Wash	29		6160.0-6161.5	155.3-156.8	—	—	—
18	29	1925	6161.5-6168.0	156.8-163.3	6.5	6.20	95
Wash	29		6168.0-6171.0	163.3-166.3	—	—	—
19	29	2200	6171.0-6176.0	166.3-171.3	5.0	4.57	91
Wash	29		6176.0-6180.5	171.3-175.8	—	—	—
20	30	0027	6180.5-6181.5	175.8-176.8	1.0	0.81	81
					167.8	165.02	98
					(total)	(total)	(avg.)

Two holes originally were scheduled for Site 578. Because of the excellent recovery and core quality in Hole 578, however, we cancelled the second hole to recover some of the time lost due to the reduced lowering speed of the HPC assembly necessitated by the undersize bore of the drill pipe.

We departed the site at 0245Z on 30 May, steaming south and streaming the seismic gear before profiling northward across the site en route to Site 579.

LITHOSTRATIGRAPHY

The lithostratigraphy of Site 578 is based on macroscopic core descriptions and smear slide analyses. The recovered section consists of four units (Fig. 1, Table 2): (1) a gray to olive gray clay-siliceous clay, (2) a yellowish brown to brown clay-siliceous clay, (3) a brown to dark brown pelagic clay, and (4) a basal chert overlain by an interbedded silicified foraminiferal ooze and clay unit.

Unit I: Gray Clay

Lithologic Unit I is a gray to olive gray clay and siliceous clay. This unit is divided into four subunits as follows.

Subunit IA

This subunit is a siliceous clay (radiolarian clay), predominantly homogeneous gray to dark gray (5Y) in color. The upper 0.71 m of this subunit is a dark yellowish brown (10YR) oxidized layer. Subunit IA extends from Section 578-1-1 through Sample 578-2-3, 20 cm (0-8.0 m sub-bottom depth). These sediments are composed of 30-60% clay, 5-10% quartz, 15-20% radiolarians, and 5-10% diatoms. This subunit contains four volcanic ash layers with an average thickness of 2.5 cm and a maximum thickness of 5 cm. Several thin (0.2-0.5 cm), indurated, dark, pyritic clay layers are found in this subunit.

Subunit IB

Subunit IB is a clay unit that extends from Samples 578-2-3, 20 cm through 578-6,CC (8.0-52.3 m sub-bot-

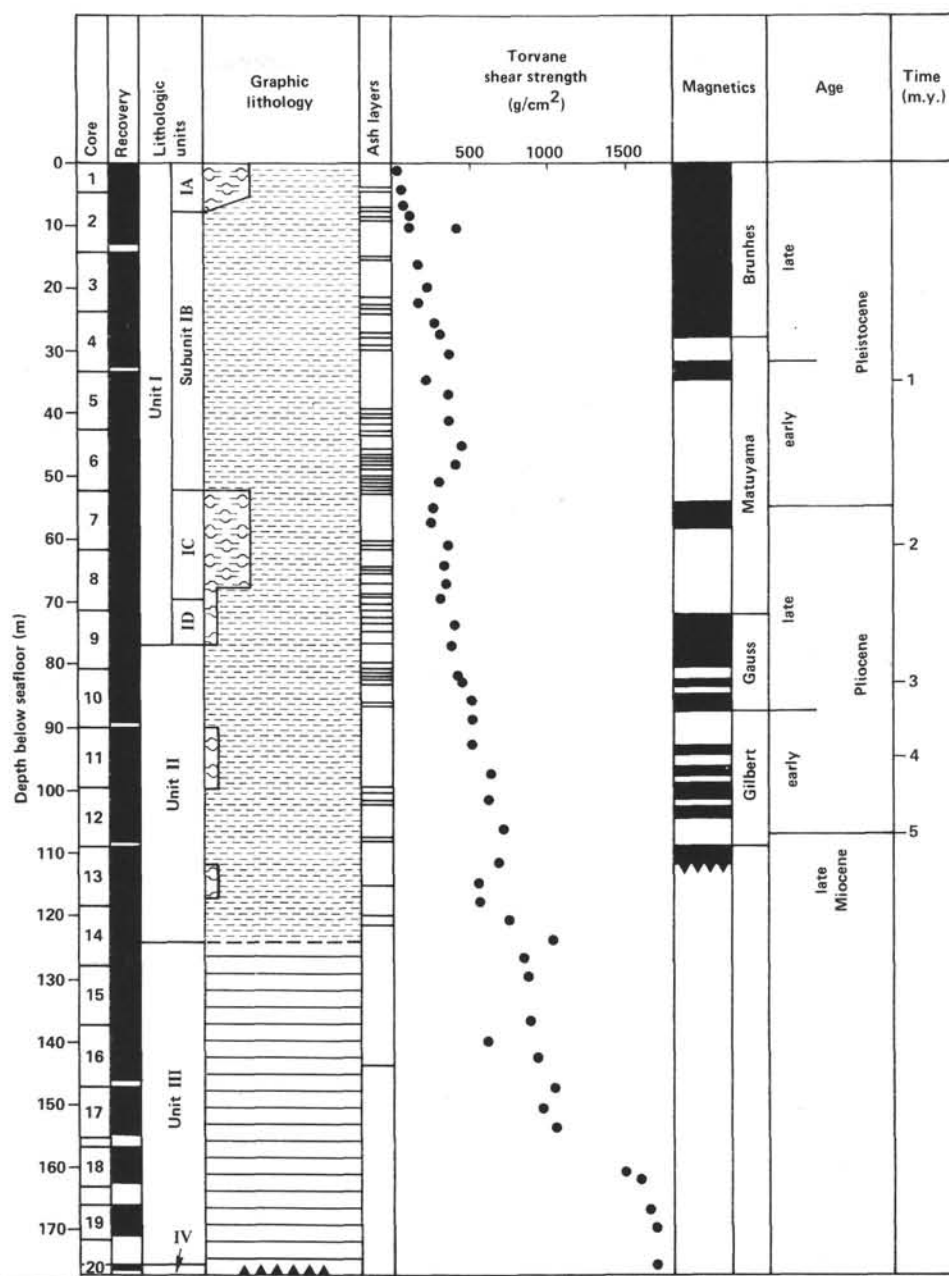


Figure 1. Site summary diagram showing Site 578 core numbers, core recovery, lithologic units, graphic lithology, ash layer locations, torvane shear strength (g/cm^2), magnetostratigraphy, and age. Symbols used in graphic lithology column are defined in Introduction and Explanatory Notes (this volume).

tom depth). In the interval from Samples 578-2-3, 20 cm to 578-4-5, 20 cm, this subunit is gray to dark gray (5Y) interlayered with olive gray; an olive gray color is predominant from Samples 578-4-5, 20 cm through 578-6, CC. The sediments are composed of 85% clay, 5–10% quartz, and generally less than 5% biogenic silica. Thirty ash layers were cored in Subunit IB. Their average thickness is 3.0 cm, with a maximum thickness of 17 cm. No ash layers were found between Samples 578-4-4, 140 cm and 578-5-5, 20 cm. Thin, stiff, dark, indurated, pyritic clay layers occur throughout the subunit, but are significantly less abundant in the interval that lacks ash layers.

Subunit IC

Subunit IC is a siliceous clay that extends from Section 578-7-1 through Sample 578-8-6, 50 cm (52.3–69.75 m sub-bottom depth). This subunit is predominantly olive gray (5Y) in color, with a few layers of green gray (5G), gray (5Y), and olive (5Y). The sediments are composed of 25–30% diatoms, 5–15% radiolarians, and 30–55% clay. The quartz content increases downsection to a maximum of 15%.

Fourteen ash layers occur in Subunit IC; the average thickness is 4.3 cm. The thickest ash layer is 12 cm. No ash layers and relatively few dark, pyritic, indurated clay

Table 2. Site 578 lithostratigraphic units.

	Lithologic unit	Cored interval	Sub-bottom depth (m)
I:	Gray to olive gray clay to siliceous clay	1-1,0 cm to 9-4,80 cm	0-76.60
	Subunit IA: Siliceous clay (radiolarian clay)	1-1,0 cm to 2-3,20 cm	0-8.00
	Subunit IB: Clay	2-3,20 cm to 6,CC	8.00-52.30
	Subunit IC: Siliceous clay	7-1,0 cm to 8-6,50 cm	52.30-69.75
	Subunit ID: Clay	8-6,50 cm to 9-4,80 cm	69.75-76.60
II:	Yellow brown to brown clay (transitional biogenic mud)	9-4,80 cm to 14-4,120 cm	76.60-124.50
III:	Brown to dark brown pelagic clay	14-4,120 cm to 20-1,20 cm	124.50-176.00
IV:	Dark brown pelagic clay and chert	20-1,20 cm to 20,CC	176.00-176.80

layers occur between Samples 578-7-1, 40 cm and 578-7-6, 70 cm.

Subunit ID

This subunit extends from Samples 578-8-6, 50 cm through 578-9-4, 80 cm (69.35-76.6 m sub-bottom depth). It consists of interbedded layers of yellowish brown to dark brown (10YR) and olive gray (5Y) clay above Sample 578-9-2, 120 cm and olive gray (5Y) and olive (5Y) clay below Sample 578-9-2, 120 cm. These sediments contain approximately 55-68% clay, 15% quartz, 5-10% diatoms, and 0-8% radiolarians. In general, the brown layers have more clay and less biogenic silica than the olive gray and gray layers.

Six ash layers are found in Subunit ID. The average thickness of these layers is 5.7 cm; maximum thickness is 10 cm. The only thin indurated, dark pyritic clay layer in this subunit occurs in Sample 578-9-2, 20 cm.

Unit II: Yellowish Brown and Brown Clay

This unit extends from Samples 578-9-4, 80 cm through 578-14-4, 120 cm (from 76.6 to 124.5 m sub-bottom depth). The upper 14 m of this unit consists of interbedded yellowish brown (10YR) and brown (10YR) clay layers 40-60 cm thick. The lower 34.5 m of this unit consists of uniform yellowish brown (10YR) clay with minor amounts of siliceous microfossils. The sediments consist of 50-89% clay, 2-20% quartz, and 2-20% biogenic silica. Isolated manganese nodules occur within this unit.

Unit II contains 19 ash layers with an average thickness of 5 cm; maximum thickness is 17 cm. The abundance of ash layers decreases rapidly below Sample 578-10-2, 30 cm. No thin, indurated, dark pyritic layers occur in Unit II.

Unit III: Dark Brown Pelagic Clay

This unit extends from Samples 578-14-4, 120 cm through 578-20-1, 20 cm (from 124.5 to 176.0 m sub-bottom depth) and consists of a uniform dark brown (10YR) to very dark grayish brown (10YR) pelagic clay. The sediment in Unit III is composed of 90% or more clay and 1-7% quartz. Biogenic silica is virtually absent through the unit. Only one ash layer occurs in Unit III.

Unit IV: Dark Brown Pelagic Clay and Chert

This unit extends from Samples 578-20-1, 20 cm through 578-20,CC (from 176.0 to 176.8 m sub-bottom depth). The top 30 cm of Unit IV consists of dark brown to brown (10YR-7.5YR) pelagic clay with laminations 0.1 to 0.5 cm thick. Below the laminated clay is a 13-cm-thick sequence of interbedded very pale brown (10YR) siliceous clay and dark grayish brown (10YR) pelagic clay. The siliceous clay contains 77% clay, 15-20% silicified foraminifers, and 3% quartz. The lowermost lithology recovered consists of angular chert fragments (Sample 578-20,CC). These chert fragments exhibit the same vitreous reddish centers and white chalky rinds described for cherts recovered elsewhere (e.g., Fischer, Heezen, et al., 1971).

SEISMIC CORRELATIONS

High resolution seismic reflection profiles (3.5 and 12 kHz) and 100-Hz reflection profiles were recorded at Site 578. Both hull-mounted and near-bottom sound sources were utilized; the near bottom transducer (3.5 and 5.25 kHz) was mounted on the drill string 251 m above the drill bit.

The 3.5-kHz echograms over Site 578 reveal a three-part seismic section (Fig. 2, Table 3). The upper Unit 1 extends to 0.0433 s below seafloor (30.7 m, assuming a velocity of 1420 m/s) and consists of strong, continuous, multiple, parallel sub-bottom reflectors. A thin transparent layer separates seismic Unit 1 from the underlying seismic Unit 2. Seismic Unit 2 consists of parallel reflectors of weak-intermediate strength and extends to 0.0641 s below the seafloor (45.5 m, assuming a velocity of 1420 m/s). A thin transparent layer separates the deepest reflector in seismic Unit 2 from the top of seismic Unit 3. Seismic Unit 3 consists of parallel multiple reflectors that are commonly intermittent and weak; only the top reflector has intermediate strength.

The source of these reflectors was difficult to determine because of (1) the high number of relatively equally spaced reflectors, (2) the best fit of reflectors to lithostratigraphy utilizes an anomalously low velocity throughout the section (1420 m/s), and (3) both ash layers and thin, indurated, pyritic clay layers have anomalously high P-wave velocities. Some of the seismically transparent intervals correspond to sections of core without ash layers but with indurated, thin pyritic clays. Therefore, we attribute most of the reflectors to ash layers (Table 3). Only Reflector 3c is probably caused by a thin, pyritic clay layer; Reflectors 2a and 2b are probably caused by locally anomalous brown clay. The remainder of the reflectors account for all the ash layers of significant thickness cored to a depth of about 70 m below the seafloor. The proposed correlation matches the ash layer stratigraphy well below seismic Unit 1d, but a mismatch above this reflector suggests (1) inaccurate interval velocities, or (2) sources other than ash layers for the reflectors, or (3) poor control on the sub-bottom depth of the cored

Diatom assemblages in Cores 4 through 7 are placed in the *N. reinholdii* Zone. Core 4 can definitely be placed

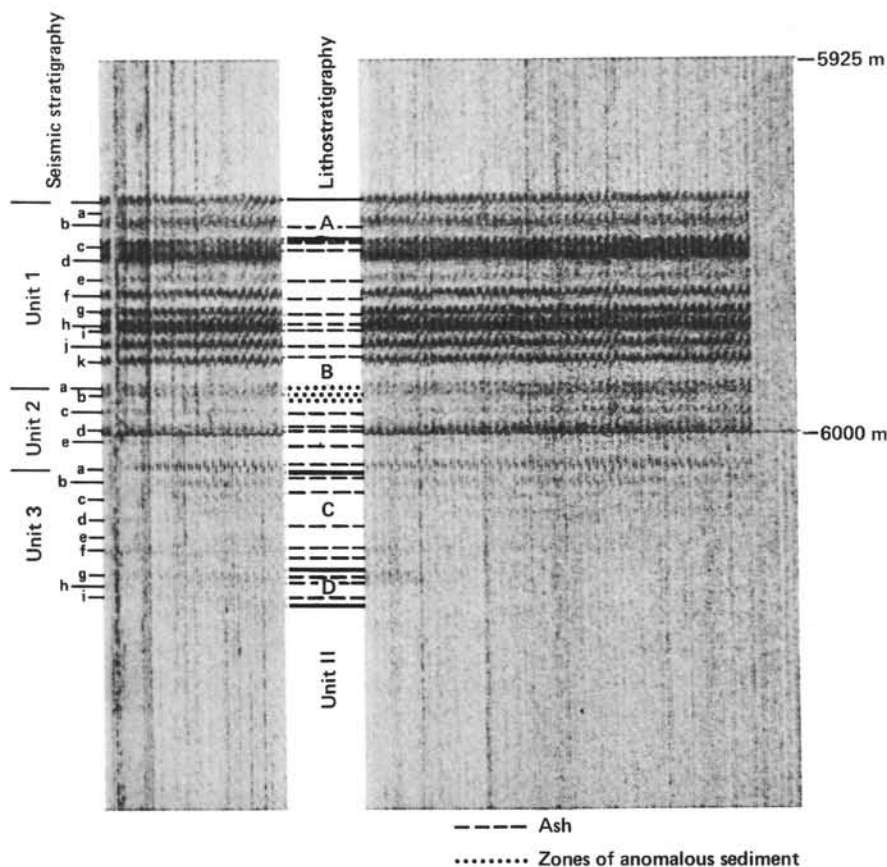


Figure 2. 3.5-kHz echogram near Site 578 showing the three-part seismic sequence described in the text.

ashes because of “intermittent flow-in” (i.e., discrete zones of “flow-in” at one or more depths within the length of a single core).

The 100-Hz seismic reflection profile over Site 578 (Fig. 3) is characterized by a three-part section. The uppermost unit (1) extends 0.23 s below the seafloor (176 m at 1520 m/s) and consists of strong, multiple sub-bottom reflectors. The strong reflectors parallel the seafloor and appear to “overprint” a few weaker, slightly divergent reflectors. Therefore, some of these strong reflectors may be “ringing” and not represent true lithologic changes. Seismic Unit 1 correlates with lithostratigraphic Units I, II, III. Seismic Unit 1 thus includes all the Cretaceous and younger sediments lying above the Cretaceous chert of lithostratigraphic Unit IV.

Seismic Unit 2 consists of strong, discontinuous, slightly divergent reflectors that form a dense “hackly” appearance on the reflection profiles. The thickness of Unit 2 is variable—from near zero on seamounts to more than 0.23 s. Unit 2 corresponds to the Cretaceous cherts and other interbedded sediments lying above basement and below lithostratigraphic Unit III.

Seismic Unit 3 consists of typical basement reflections and occurs at variable depths (less than 0.03 s on the slopes of seamounts, to about 0.5 s [378 m at 1520 m/s] elsewhere) below the seafloor.

BIOSTRATIGRAPHY

The sediments recovered at Site 578 range in age from late Quaternary to Late Cretaceous. No nannofossils were found except a few specimens in Section 578-16-2 which do not allow any age assignment. The sediments were also barren of foraminifers except for Samples 578-18, CC (18–20 cm), 578-20-1, 64–66 cm and 578-20, CC. The foraminifers found in Core 18 are of early middle Eocene age whereas the samples from Core 20 contained an upper Campanian to Maestrichtian assemblage. Ichthyoliths in Samples 578-17-4, 140–150 cm and 578-19-2, 140–150 cm have tentatively been dated as early Oligocene and Eocene in age, respectively. The upper 128 m of cored sediments contained rare to abundant diatoms and radiolarians varying in degree of preservation from good to poor.

No major hiatuses were detected in the late Miocene through Quaternary sequence. The absence of siliceous or calcareous microfossils through most of the interval between 125 and 175 m (Cores 14 through 19) at this site precludes the identification of any gaps in the record over this period. Based on the radiolarian and diatom biostratigraphy (Fig. 4), the Pliocene/Pleistocene boundary lies near the base of Core 7, with the Miocene/Pliocene boundary present in Core 12.

Table 3. 3.5-kHz seismic correlations, Site 578.

Reflector	Relative strength ^a	Sub-bottom depth (s)	Sub-bottom depth ^b (m)	Depth below seafloor of corresponding lithology (m)	Source
1a	W	0.00269	1.91		
1b	I	0.00608	4.32	4.75	Ash #2
1c	VS	0.0120	8.52	7.6?	Ash #3
1d	VS	0.0153	10.86	8.9	Ash #5
				9.1	Ash #6
1e	W	0.021	14.91	15.0	Ash #7
1f	S	0.025	17.75	18.75	Ash #8
1g	S	0.0302	21.44	21.5	Ash #9
1h	VS	0.0331	23.50	23.0	Ash #10-#11
1i	VS	0.0353	25.06	24.0	Ash #12
1j	S	0.0391	27.76	27.5	Ash #13
1k	S	0.0433	30.7	29.5	Ash #15-#16
2a	W	0.0496	35.2	34.5	Brown pelagic clay
2b	W	0.0516	36.6	35.6-36.75	Brown pelagic clay
2c	IT-W	0.0560	39.8	40.0	Ash #16A-#18
2d	I-S	0.0610	43.3	42.75	Ash #20
				43.3	Ash #21
2e	IT	0.0641	45.5	46.4	Ash #23
				46.6	Ash #24
3a	I	0.0713	50.6	50.2	Ash #29-#32
3b	IT	0.0744	52.8	52.5	Ash #35-#37
3c	IT	0.0786	55.8	55.0-55.75	Pyritic, indurated clay
3d	IT-W	0.0847	60.1	61.3	Ash #38-?#42
3e	IT	0.0905	64.25	65.2	Ash #43-#45
3f	IT-W	0.0930	66.0	67.2	Ash #46
3g	IT-W	0.0992	70.4	71.5	Ash #50
3h	IT	0.1025	72.8	72.45	Ash #51
3i	IT	0.1054	74.8	74.75	Ash #53
3j	IT	0.143	101.5	101.6	Ash #65 and #66

^a IT = intermittent, weak; W = weak, but generally continuous; I = intermediate; S = strong; VS = very strong.
^b Assuming a velocity of 1420 m/s.

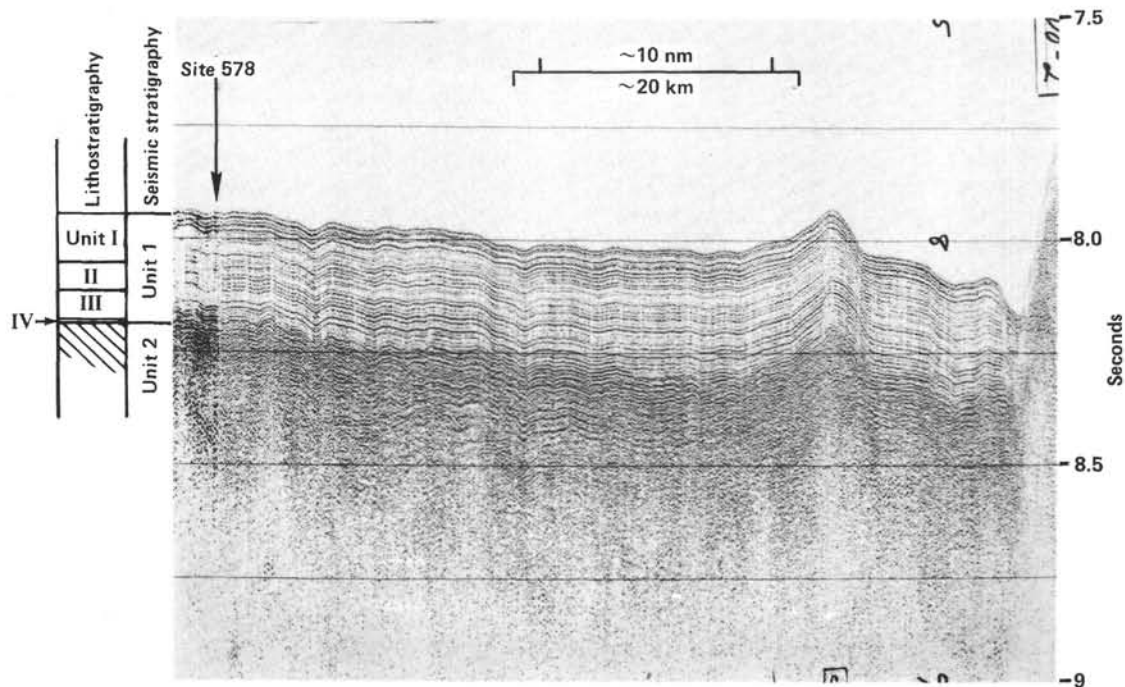


Figure 3. 100-Hz reflection profile over Site 578 showing the three-part seismic sequence described in the text.

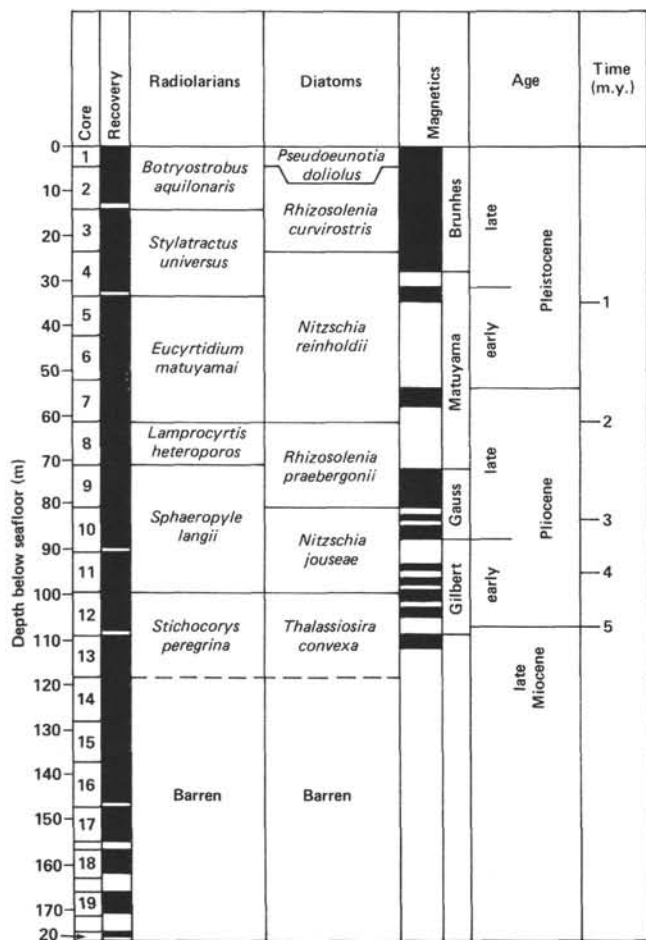


Figure 4. Site 578 biostratigraphic and magnetostratigraphic summary.

Calcareous Nannofossils

No calcareous nannofossils were found in cores recovered from this site with the exception of one assemblage in Sample 578-16-2. Rare and poorly preserved specimens include *Watznaueria barnesae*, *Braarudosphaera bigelowi*, *Zygodiscus* sp., *Coccolithus pelagicus*, *Coccolithus* sp., and *Discoaster* sp.

Planktonic Foraminifers

Core-catcher samples were examined from all 20 cores recovered at Site 578. In addition, two samples (578-16-5, 7-8 and 138-139 cm) from light colored layers within the dark pelagic muds were examined on board. Shore-based analysis revealed foraminifers in Samples 578-18, CC (18-20 cm) and 578-20-1, 64-66 cm. All samples except these two and Sample 578-20, CC (examined aboard ship) were barren of foraminifers. Sample 578-18, CC (18-20 cm) contained rare specimens of *Globorotalia spinulosa* and *G. broedermanni*. These two species alone indicate an interval spanning the *G. pentacamerata* Zone to the *Globigerinatheca subconglobata* Zone of Stainforth et al. (1975) or P9-P11 of Blow (1969). The samples from Core 20 contained a fauna of upper Campanian to Maestrichtian age. Typical species include *Globotruncana contusa*, *G. arca*, *G. fornicata*, *G. tricarinata*, *G. stu-*

arti, *G. stuartiformis*, *G. lapparenti*, *Heterohelix striata*, *Hedbergella planispira*, *Globigerinelloides asperus*, *G. prairiehillensis*, and *Rugoglobigerina rugosa*. These forms are common to the Upper Cretaceous as reported by Olsson (1964), Pessagno (1967), and Postuma (1971). The fauna found in Core 20 is similar in age to that found just above the impenetrable chert layer at Site 576, with the addition of some Maestrichtian forms. At Site 578, however, all the specimens were silicified after undergoing some dissolution. Such silicification was not seen at Site 576.

Radiolarians

Sediments from Site 578 contain Quaternary through late Miocene radiolarians. The preservation of individual specimens varied from good to poor in Samples 578-1, CC through 578-13, CC. No radiolarians were found in core-catcher samples from Cores 14 through 20. The radiolarian biostratigraphy for Site 578 is shown in Figure 4.

Radiolarians representative of the late Pleistocene are present in samples 578-1, CC through 578-4, CC with the first 14 m (Cores 1 and 2) at Site 578 containing an assemblage characteristic of the *Botryostrobus aquilonaris* Zone (Hays, 1970). The presence of *Stylatractus universus* and the absence of *Eucyrtidium matuyamai* in Samples 578-3, CC and 578-4, CC indicate that sediments recovered in this interval correlate with the *Stylatractus universus* Zone (Hays, 1970). The identification of the radiolarian species *E. matuyamai* in Samples 578-5, CC through 578-7, CC indicates that the sediments in these cores are early Pleistocene in age. Because of the relatively small width of the *E. matuyamai* specimens in Sample 578-7, CC, which is indicative of the beginning of its lineage, the Pliocene/Pleistocene boundary is probably very close to the bottom of Core 7. The species in Sample 578-8, CC are a typical late Pliocene assemblage characteristic of the *Lamprocyrtis heteroporos* Zone (Hays, 1970; Foreman, 1975). The presence of *Stichocorys peregrina*, *S. delmontensis*, and *Sphaeropyle langii* in Samples 578-9, CC through 578-11, CC indicate that this sequence belongs to the *S. langii* Zone (Foreman, 1975). Species characteristic of the *Stichocorys peregrina* Zone (Riedel and Sanfilippo, 1970; Foreman, 1975) are present in Samples 578-12, CC and 578-13, CC with the Miocene/Pliocene boundary occurring within Core 12.

Diatoms

Early Pliocene to Quaternary diatoms were recovered at Site 578 (Fig. 4). Diatoms are common to few and preservation is moderate except for Cores 5 and 13 where diatoms are rare and poorly preserved. Diatoms are absent below Core 13. Core 1 belongs to the lower latitude *Pseudoeunotia doliolus* Zone of Burckle et al. (1978) and the higher latitude *Denticulopsis seminae* Zone of Koizumi (1973) based upon the absence of *Rhizosolenia curvirostris*. Cores 2 and 3 are placed in the middle Pleistocene *R. curvirostris* Zone (the middle and lower part of the Brunhes Epoch) by the presence of *P. doliolus* and *R. curvirostris* and the absence of *Nitzschia reinholdii*.

around the Jaramillo Event of the Matuyama Epoch. The silicoflagellate *Mesocena quadrangula* is present in this core. The stratigraphic position of the base of Core 5 is less certain because of poor preservation. The top of Core 5 (Section 578-5-1) is near the Jaramillo Event, based upon the presence of *Rhizosolenia matuyamai* which ranges into the lower part of the Jaramillo.

Cores 8 and 9 are placed in the uppermost part of the Pliocene *R. praebergonii* Zone, based on the presence of *Thalassiosira convexa* and the absence of *Nitzschia jouseae*. Core 9 bottoms in the upper part of the Gauss Epoch as indicated by the presence of *T. convexa* and the absence of *N. jouseae* and *Denticulopsis kamtschatica*. Cores 10 and 11 are placed in the early to middle Pliocene *N. jouseae* Zone based upon the co-occurrence of *N. jouseae* and *T. convexa*. Core 12 is placed in the *T. convexa* Zone (magnetic Epoch 5) by the presence of *Nitzschia miocenica*, *T. convexa*, and *T. miocenica*. The Miocene/Pliocene boundary, therefore, lies between Cores 11 and 12 based on the occurrence of *N. miocenica* and *T. miocenica*. Core 13 is also placed in the *T. convexa* Zone (uppermost part of magnetic Epoch 6) by the co-occurrence of *T. convexa* and *T. praeconvexa*.

Ichthyoliths

Samples were taken from Cores 578-11 through 578-19 for a preliminary investigation of ichthyoliths. Ichthyoliths range in abundance from rare in the late Miocene-Pliocene siliceous sediments (Cores 578-11 through 578-13) to very abundant in pelagic clays of the Oligocene (Section 578-17-5) and the Paleocene/Eocene boundary (Core 578-19).

Core 578-12 through Section 578-17-4 is judged to be Miocene on the basis of the coherent range of *Small triangle long striations*. Section 578-14-2 is late Miocene on the basis of the concurrence of *Long triangle short inline* and *Long ellipse*. The presence of *Circular with line across* and *Short rectangular with striations* in Section 578-16-2 indicates a middle Miocene age.

The Oligocene/Miocene boundary falls between Sections 578-17-4 and 578-17-5; the Eocene/Oligocene boundary between Sections 578-17-5 and 578-18-1. The Oligocene is identified on the presence of *Rounded apex triangle* and *Triangle with base angle* and the absence of *Small triangle long striations*. It is not possible to tell from the available data whether some part of the Oligocene and early Miocene is missing or if sediment accumulation was very slow.

Core 578-18 and Section 578-19-1 are Eocene. On the basis of the absence of *Triangle curved based* in the top part of the sequence and its presence in the bottom, Sections 578-18-1 and 578-18-3 are middle to late Eocene. Section 578-18-4 and Section 578-19-1 are early to middle Eocene.

The Paleocene/Eocene boundary is between Sections 578-19-1 and 578-19-3. The presence of *Beveled triangle concave margins* in Section 578-19-2, as well as *Triangle radiating inline* and *Narrow straight triangle* suggests that this section is Paleocene, but the distribution of typically Paleocene forms in earliest Eocene has not been

studied sufficiently to allow a confident Paleocene age assignment to this sample. The presence of *Triangle medium wing* and *Triangle curved base* in Section 578-19-3, together with the Paleocene forms listed above, indicates a late Paleocene age.

PALEOMAGNETICS

Excellent recovery of an undisturbed section with NRM intensities on the order of 50×10^6 G allowed us to establish a nearly complete magnetostratigraphy from the late Miocene to the Quaternary at this site.

Detailed shore-based magnetic results are described in a later chapter (see Heath, Rea, and Levi, this volume). The average NRM inclinations above 110 m are independent of the polarity and are close to the centered axial dipole value for the present latitude of the drill site (53°). Thus, they can be used to establish the polarity sequence down to Epoch 5 (Table 4), using the magnetic terminology of McDougall (1977).

SEDIMENT ACCUMULATION RATES

The sedimentation rates for this site are based on a combination of radiolarian, diatom, ichthyolith, foraminiferal, and paleomagnetic stratigraphies. In constructing the age-depth plot (Fig. 5), it is assumed that the Campanian-Maestrichtian silicified foraminiferal sediments found below 175 m are contemporaneous with the clays directly overlying them. Sedimentation rates during the late Pleistocene decreased from almost 40 m/m.y. at the surface to less than 30 m/m.y. at depth. Rates were close to 25 m/m.y. during the early Pleistocene and late Pliocene (Figs. 5 and 6). Early Pliocene rates de-

Table 4. Paleomagnetic reversals at Site 578 (shipboard NRM inclinations).

Age ^a (m.y.)	Age ^b (m.y.)	Age ^c (m.y.)	Depth in hole (m)	Boundary/Event
0.73	0.72	0.72	26.9	Brunhes/Matuyama
0.91	0.91	0.89	31.8	Jaramillo
0.98	0.97	0.94	34.5	
1.66	1.66	1.62	54.2	Olduvai
1.88	1.87	1.91	58.0	
	2.12	2.07	61.7	X (Reunion)
	2.14		62.1	
2.47	2.47	2.47	72.9	Matuyama/Gauss
2.92	2.91	2.91	80.4	Kaena
2.99	2.98	3.00	82.4	
3.08	3.07	3.07	83.6	Mammoth
3.18	3.17	3.17	85.0	
3.40	3.40	3.41	87.7	Gauss/Gilbert
3.88	3.86	3.82	93.4	Cochiti
3.97	3.98	3.92	94.7	
4.10	4.12	4.07	96.4	Nunivak
4.24	4.26	4.25	97.7	
4.40	4.41	4.44	99.1	Sidufjall
4.47	4.49	4.57	101.6	
4.57	4.59	4.72	102.6	Thvera
4.77	4.79	4.94	104.6	
5.35	5.41	5.44	109.0	Gilbert/Epoch 5

^a Time scale of Berggren et al. (in press).

^b Time scale of Ness et al. (1980).

^c Time scale of McDougall (1977).

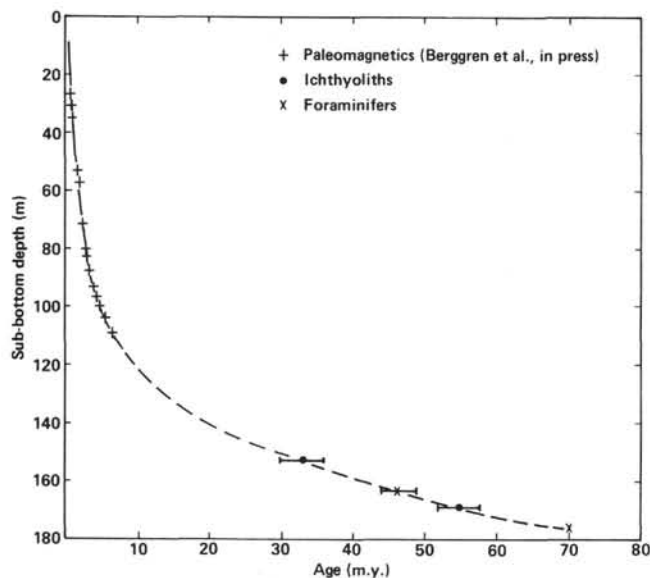


Figure 5. Age-depth curve for Site 578.

creased to less than 12 m/m.y. The very dark brown pelagic clay below 130 m accumulated at an average rate of 0.8 m/m.y., 50 times slower than the late Quaternary deposits. The oldest deposits (170–180 m) accumulated at the lowest rates (approximately 0.45 m/m.y.).

A marked increase in sedimentation rate occurs in the late Miocene–early Pliocene if the time scale of Berggren et al. (in press) for the magnetic event is adopted. The ages assigned to these events by McDougall (1977) produce a curve that indicates a more uniform decrease in the sedimentation rate through this interval.

PHYSICAL PROPERTIES

Physical properties measurements at Site 578 were performed using mainly standard Deep Sea Drilling Project (DSDP) methods (Boyce, 1976a, b; see Introduction and Explanatory Notes, this volume). Table 5 summarizes the properties that were measured at Hole 578. Measurements were taken at approximately 3-m intervals through Hole 578. Figures 7, 8, and 9 show profiles of compressional and shear wave velocity, saturated bulk density and water content, and shear strength, respectively. A full discussion of the physical properties of the recovered sediment, including tables of the data, is given by Schultheiss (this volume). However, some of the more interesting features of the data are highlighted here.

1. The compressional wave profile (Fig. 7) is dominated by high velocity layers of pyrite-indurated clay and ash beds superimposed on a constant velocity profile down to 160 m. Not all of the numerous layers were measured, but it can be assumed that they all have higher velocities. Below 160 m there is an indication that a

Table 5. Physical properties measurements made at Site 578.

	Hole 578
Shear strength:	
Hand-operated vane	x
Motorized vane	x
Wave velocity:	
Shear wave	x
Compressional wave	x
Water content/bulk density:	
Shipboard analysis	x
Shore-based analysis	x
Bulk density by 2-min. GRAPE	x

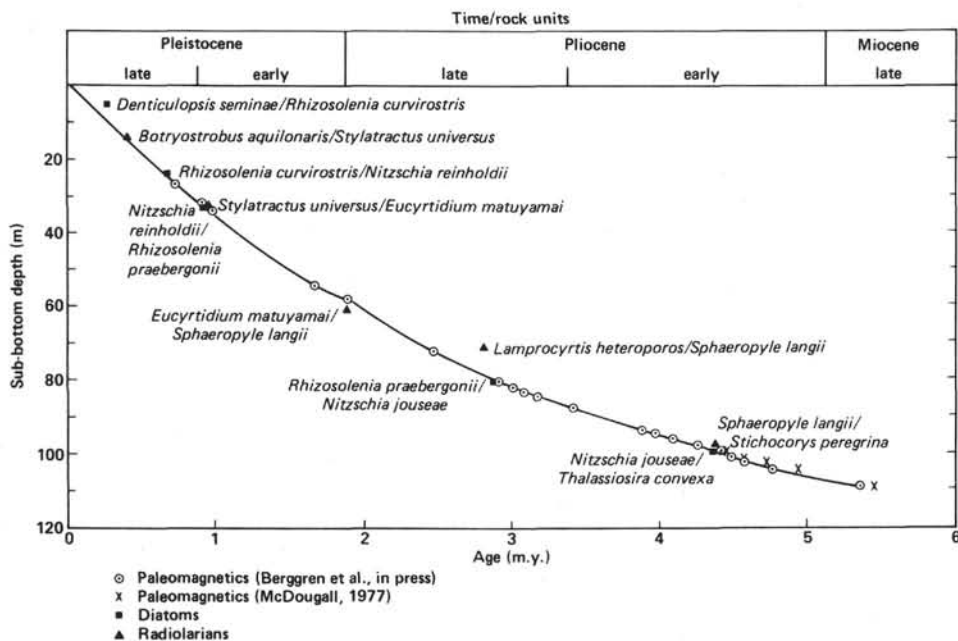


Figure 6. Age-depth curve for the upper 110 m at Site 578.

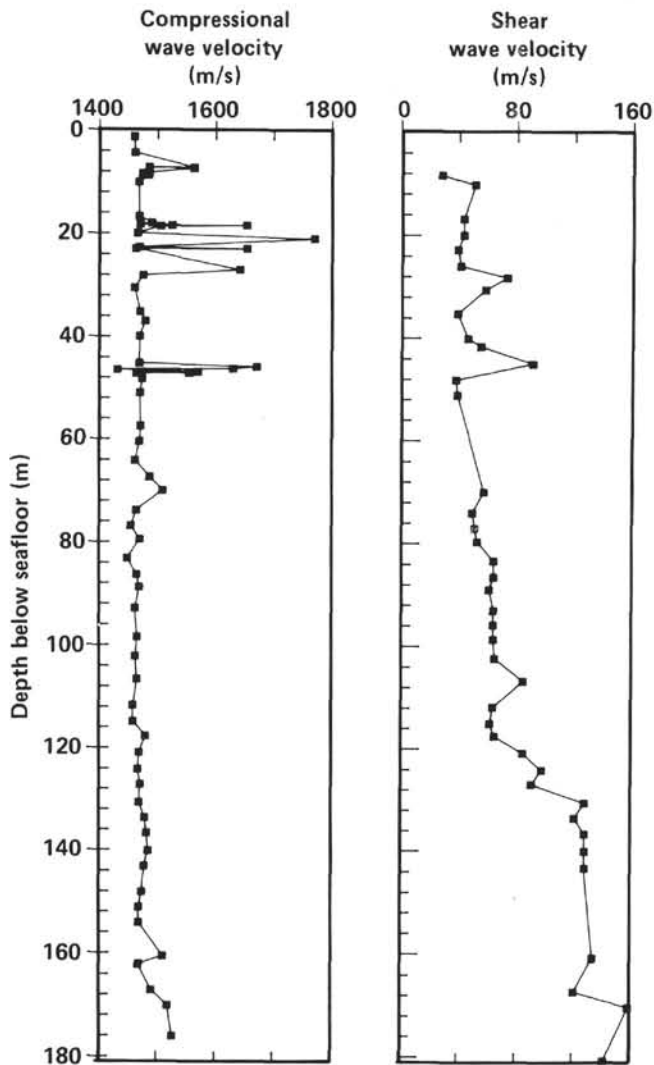


Figure 7. Plot of compressional and shear wave velocities versus sub-bottom depth at Site 578.

positive velocity gradient is developing in the very dark pelagic clay.

2. Shear wave velocities increase slowly up to 65 m/s at a depth of 120 m (Fig. 7). A rapid increase up to 128 m/s occurs between 120 and 130 m, below which the velocity remains essentially constant. This transition coincides with the lithologic boundary between Units II (clay) and III (pelagic clay).

3. The lithologic boundary between Units II and III is also characterized by a reduction in water content from 120 to 90% with a corresponding increase in the bulk density from 1.37 to 1.47 g/cm³ (Fig. 8). Another significant change in water content occurs between Cores 17 and 18 (155–160 m sub-bottom depth) where it falls rapidly from 90 to 60%. This transition does not coincide with any obvious lithological boundary.

4. The shear strength profiles (Fig. 9) show the strength increasing with depth from 0 at the seafloor to around 1500 g/cm² at 176 m in Core 20. Recovery from Cores 17, 18, 19, and 20 were progressively poorer, with Core

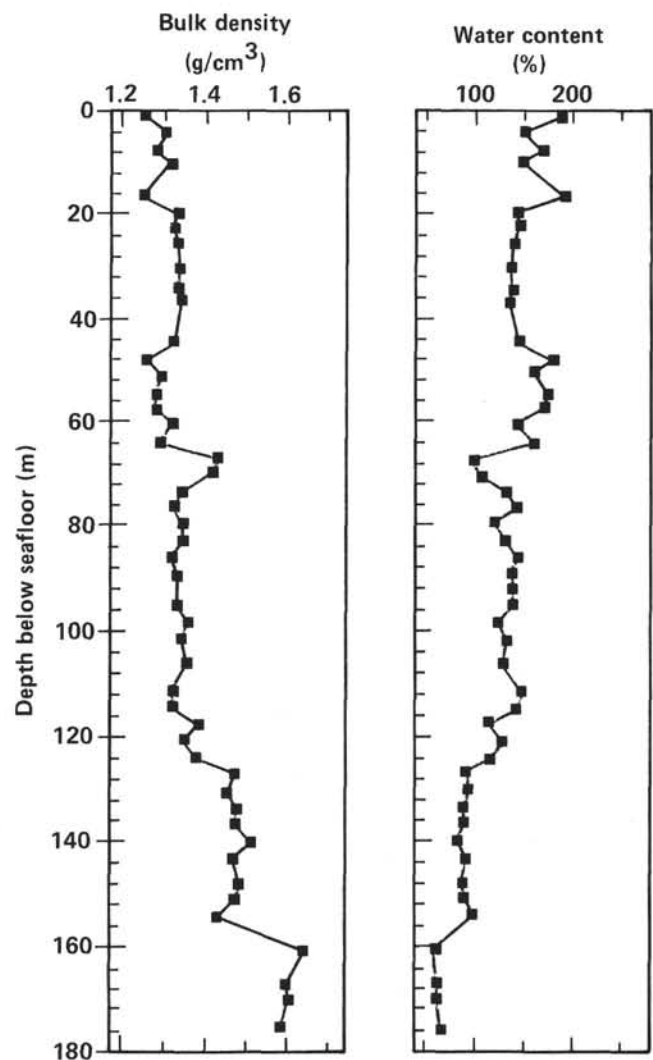


Figure 8. Profiles of saturated bulk density and water content versus sub-bottom depth at Site 578.

20 being only 0.81-m long. These shear strengths in pelagic brown clays obviously represent the operational limits of the HPC in its present configuration. It is also interesting to note that the high lateral stresses within the core prevented any flow-in occurring (presumably water must have flowed around the piston during pull out).

The two discontinuities of water content at 120–130 and 155–160 m discussed above are also revealed by rapid increases in the shear strength profiles. At 123 m (boundary of Units II/III) there is a rapid increase from 500 to 1100 g/cm² according to the motorized vane measurements (a less pronounced step is revealed by the hand-held vane). At 157 m the hand-held vane shows an increase from 1050 to 1500 gm/cm² (a less pronounced step is revealed in this case by the motorized vane).

INORGANIC GEOCHEMISTRY

Six squeezed core samples from Hole 578 were analyzed for the standard suite of components: pH, alkalinity, salinity, calcium, magnesium, and chlorinity (Ta-

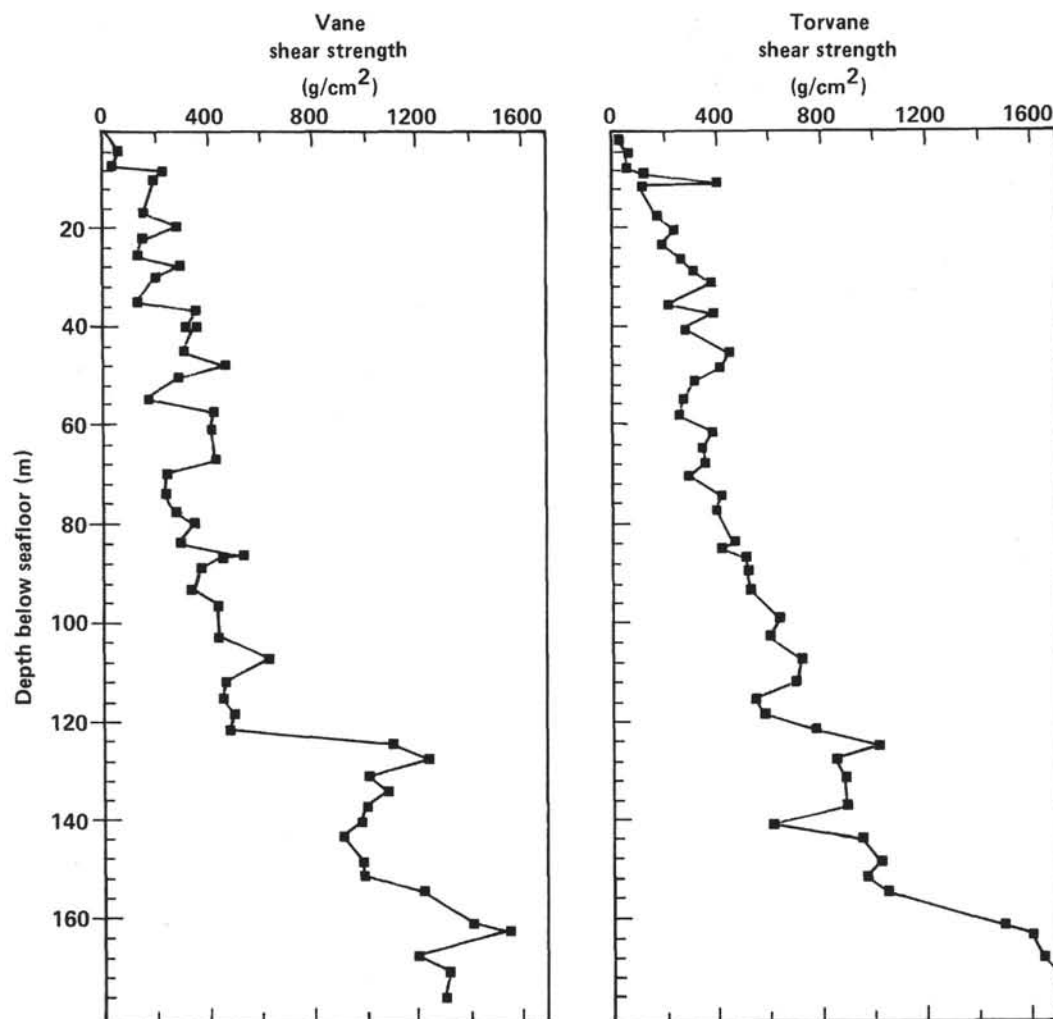


Figure 9. Plot of shear strength versus sub-bottom depth at Site 578.

ble 6). No *in situ* samples were taken. At least three trends are evident (Fig. 10):

1. Calcium increases linearly with depth throughout the cored interval. We suspect that this is a diffusion profile between the carbonate section beneath the chert (as sampled at Site 304, for example) and the seafloor.

2. Alkalinity and pH decrease within the anoxic sediments above 76 m (and possibly in the uppermost oxidized siliceous clays, although our sample spacing cannot resolve this), but are virtually constant in the highly oxidized pelagic clay section. Sulphide oxidation and alteration of volcanic ashes are reactions in the reduced

sediments that could affect these parameters. The slight increase in alkalinity at 150 m may reflect the influence of carbonate dissolution beneath the cored section.

3. The slight decrease in magnesium in the upper 70 m (in the reduced sediments) may again reflect the alteration of the abundant volcanic ash in this section to smectite. Diagenesis of biogenic opal would have a similar effect.

We have no explanation for the low salinity value at 128 m.

HEAT FLOW

Downhole temperature measurements using the new Woods Hole Oceanographic Institution (WHOI) heat flow instrument were made at this site. All but one of eight deployments were successful. The failure of the eighth run at this site was attributed to a malfunction of the computer when loading the program. All runs were made by one recorder, WHOI-4A, connected to battery pack NTLT-2.

The quality of the temperature data improved substantially at this site, owing mainly to the Cruise Operations Manager's suggestion that tension in the sand line

Table 6. Inorganic geochemistry measurements made at Site 578.

Sample	pH	Alkalinity (mEq/l)	Salinity (‰)	Calcium (mM)	Magnesium (mM)	Chlorinity (‰)
IAPSO	8.00	2.47	35.2	10.55	53.99	19.38
SSW	8.01	2.37	35.2	10.49	53.93	18.48
578-2-5, 140-150 cm	7.75	3.91	35.5	11.33	49.95	19.24
578-5-6, 140-150 cm	7.84	3.36	35.5	12.26	49.08	19.31
578-8-5, 140-150 cm	7.40	2.42	35.5	12.93	47.93	19.18
578-11-6, 140-150 cm	7.11	1.87	35.5	13.43	47.85	19.24
578-14-6, 140-150 cm	7.01	1.88	34.6	14.46	49.11	18.91
578-17-3, 140-150 cm	7.06	2.35	35.2	15.15	47.33	19.11

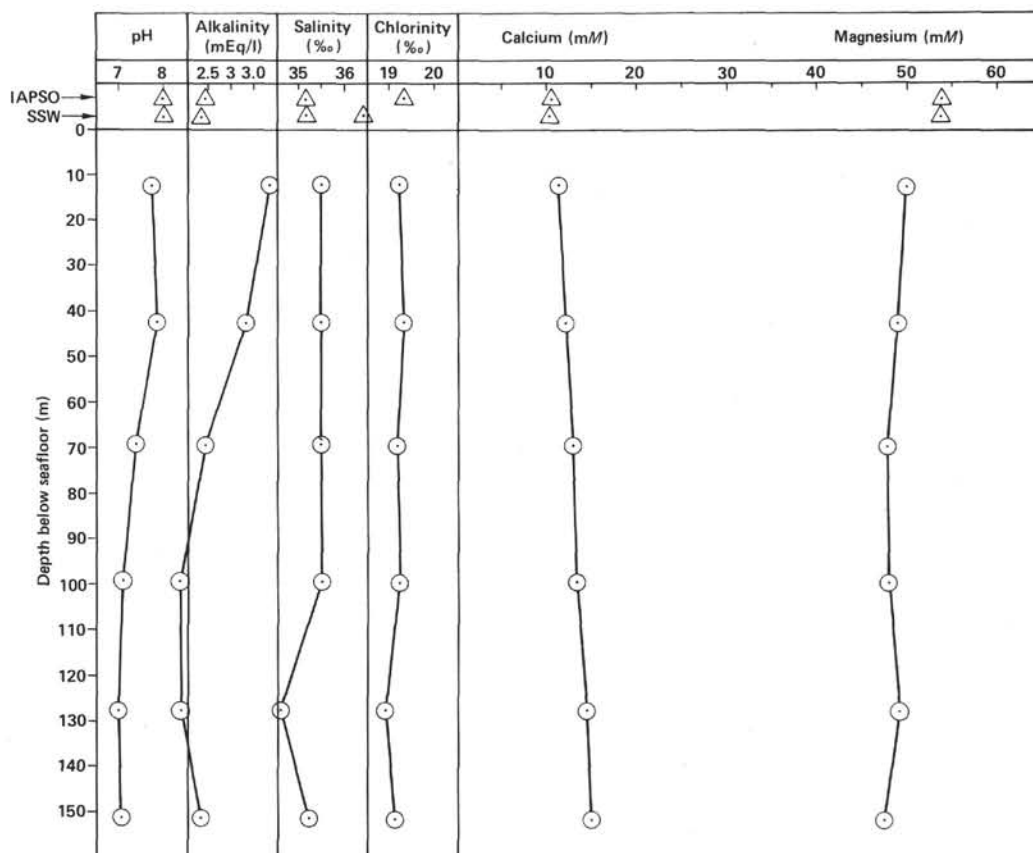


Figure 10. Profiles of pH, alkalinity, salinity (‰), chlorinity (‰), calcium (mM), and magnesium (mM) versus sub-bottom depth from interstitial water samples analyzed at Site 578. Symbols are as follows: Δ = IAPSO and SSW standards; \circ = samples from Hole 578.

be released during the measurement. This eliminated propagation of the ship's motion through the sand line to the HPC (which generates frictional heat) resulting in a smoother cooling curve than in previous records.

Thermal conductivity values were measured at 200 locations in Hole 578. These data, combined with the down-hole temperature measurements, yield a useful estimate of the heat flow at Site 578 (see Horai and Von Herzen, this volume).

SUMMARY AND CONCLUSIONS

The stratigraphic section recovered in Hole 578 and the major lithologic units, summarized in Figure 1, are as follows.

Unit I: 0–76.6 m

Gray and olive gray anoxic clay grading to siliceous clay, of late Pliocene and Quaternary age (0–2.4 m.y.). There are thin oxidized layers at the surface, at 35 and at 70 m. Siliceous microfossils are most abundant in the latest Quaternary and late Pliocene to early Pleistocene deposits (preservation also is good across the Miocene/Pliocene boundary). The youngest sediments accumulated at almost 40 m/m.y., but from about 1 to 2.4 m.y. ago, the rate was close to 25 m/m.y. This unit contains numerous ash beds (Fig. 1).

Unit II: 76.6–124.5 m

Mainly yellow brown, with some brown above 90 m, oxidized pelagic clay with locally abundant radiolarians and diatoms, of late Miocene to late Pliocene age (2.4 to about 9 m.y.). Below 90 m, the sediments are very uniform in appearance, with only ash beds (decreasing down-section) and rare ferromanganese nodules to break the monotony. Within this unit, the accumulation rate decreases steadily from 14 m/m.y. at the top to about 5 m/m.y. at the base.

Units I and II carry a strong remanent magnetization. Based on shipboard NRM analyses, the first four magnetic epochs and virtually all their events can be recognized (Fig. 4). The paleomagnetic data, which are consistent with the biostratigraphy, provide a detailed time scale for the past 5 m.y.

Unit III: 124.5–176 m

Mainly dark to very dark brown, fine-grained ("slick"), homogeneous pelagic clay, with dark yellow brown and yellow brown intervals above 129 m. The age limits of about 9 and 70 m.y. are defined by the bounding units; no diagnostic siliceous or calcareous microfossils occur near the boundaries of Unit III. This highly oxidized unit contains rare ferromanganese nodules and only one

ash bed. If deposition was continuous, the sedimentation rate decreased from 4.3 m/m.y. at the top to 0.45 m/m.y. at the base. More detailed studies of ichthyoliths are needed to determine whether this rate varied uniformly through time.

Unit IV: 176.8 m

Hole 578 terminated in chert. The few fragments in the catcher of Core 20 consist of glassy flintlike chert and light gray porcellanite containing internal molds and quartz replacements of Campanian to Maestrichtian foraminifers. The age of this chert is close to that at Site 576, but may be slightly younger.

Lithologic Unit I is problematic. The very high deposition rate, which decreases very rapidly to the southeast (*Vema-36* Cores 41PC, 44PC, and 45PC) is not due to a flood of biogenous opal, but rather to terrigenous debris. Whether this reflects near-bottom circulation (we may be seeing the initiation of a "drift" deposit), or the injection of large amounts of loess to the western North Pacific by east Asian rivers following the onset of northern hemisphere glaciation, is unclear. Shore-based grain size and mineralogical studies may throw light on this question.

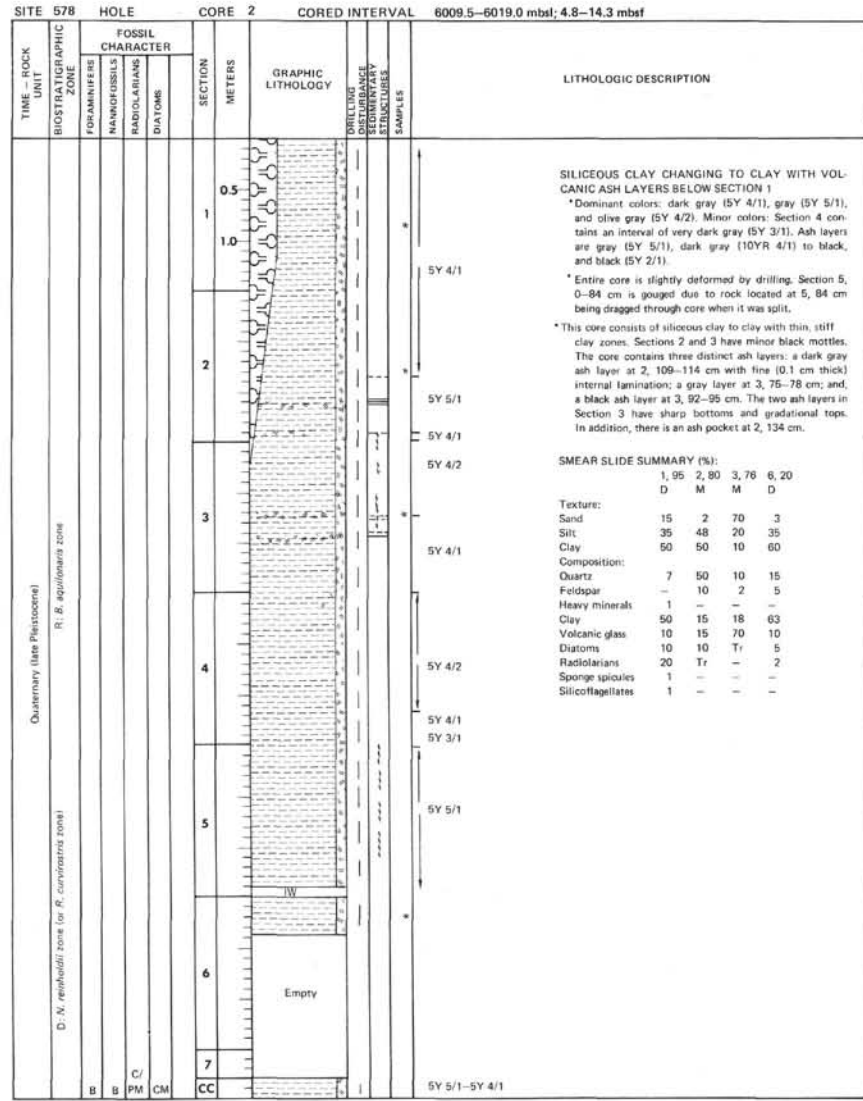
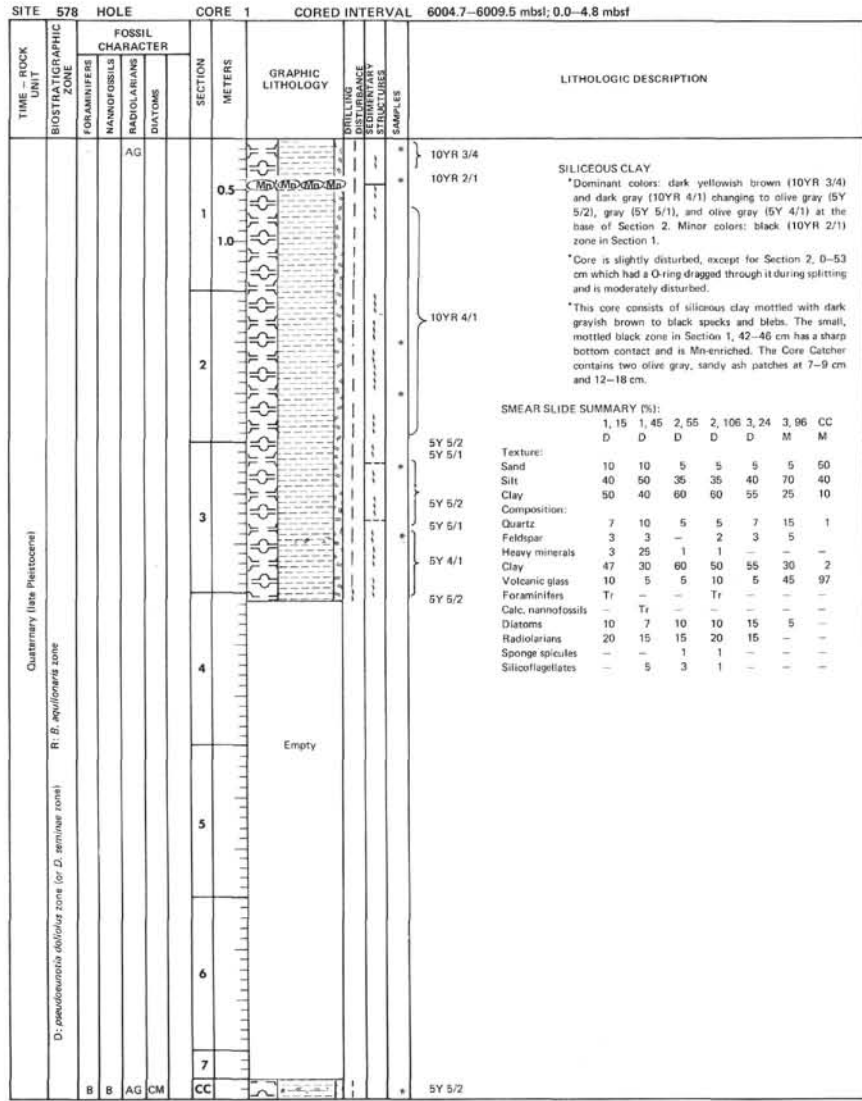
The excellent paleomagnetic record induced us to critically compare the time scale of McDougall (1977) with those of other authors. The differences are small, but our data are better fitted by the McDougall values, particularly for the top of the Olduvai Event and for the boundaries of the Sidufjall and Thvera Events. We have used McDougall's dates for our sedimentation rate calculations.

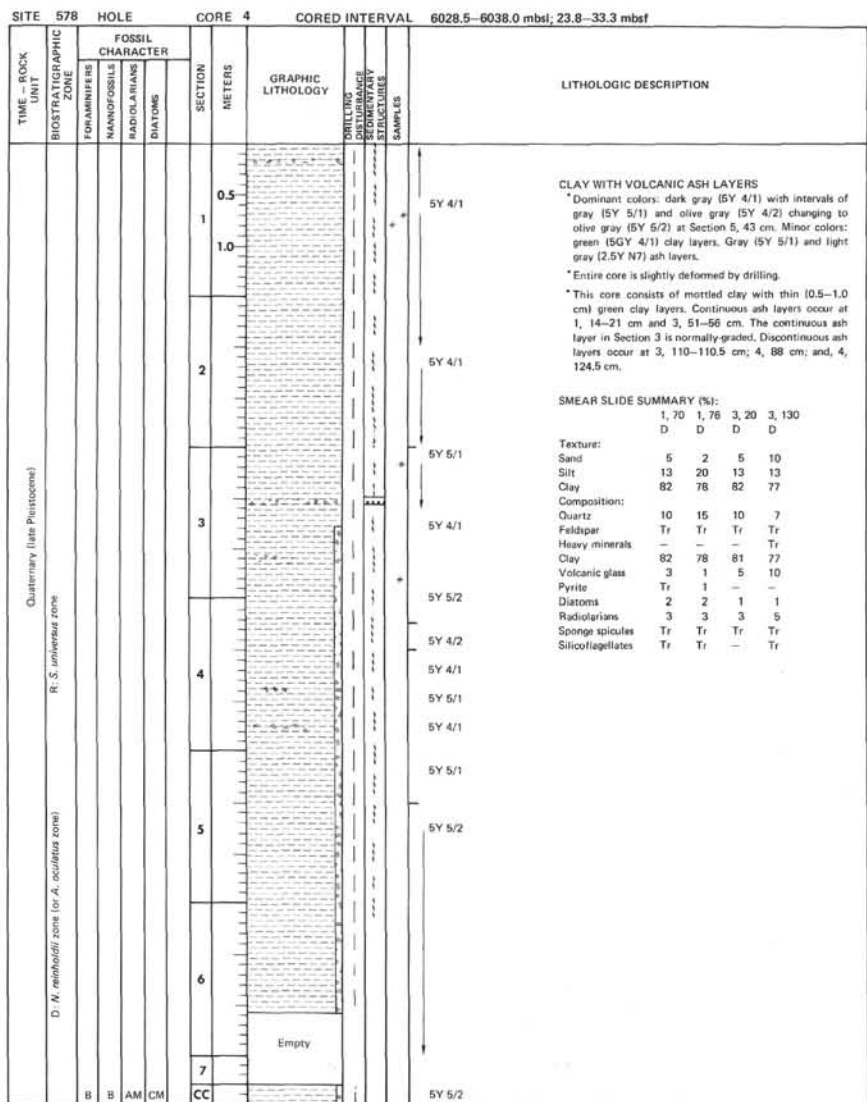
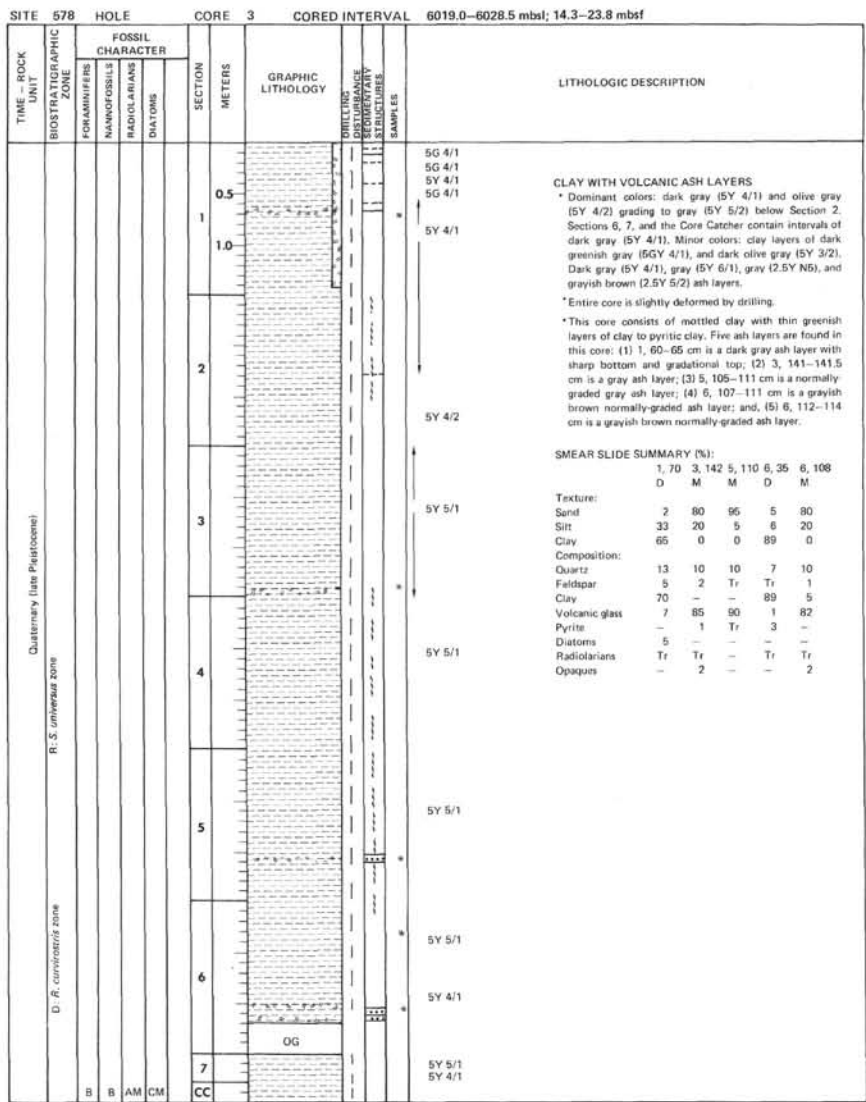
Lithologic Units II and III are comparable to units at Site 576. Unit III is manganese rich and we infer that it includes a substantial authigenic component. Unit II reflects the onset of biosiliceous deposition as the site began to encounter the western boundary current system of the North Pacific. This unit also may have received more eolian material as the climate deteriorated during the late Neogene.

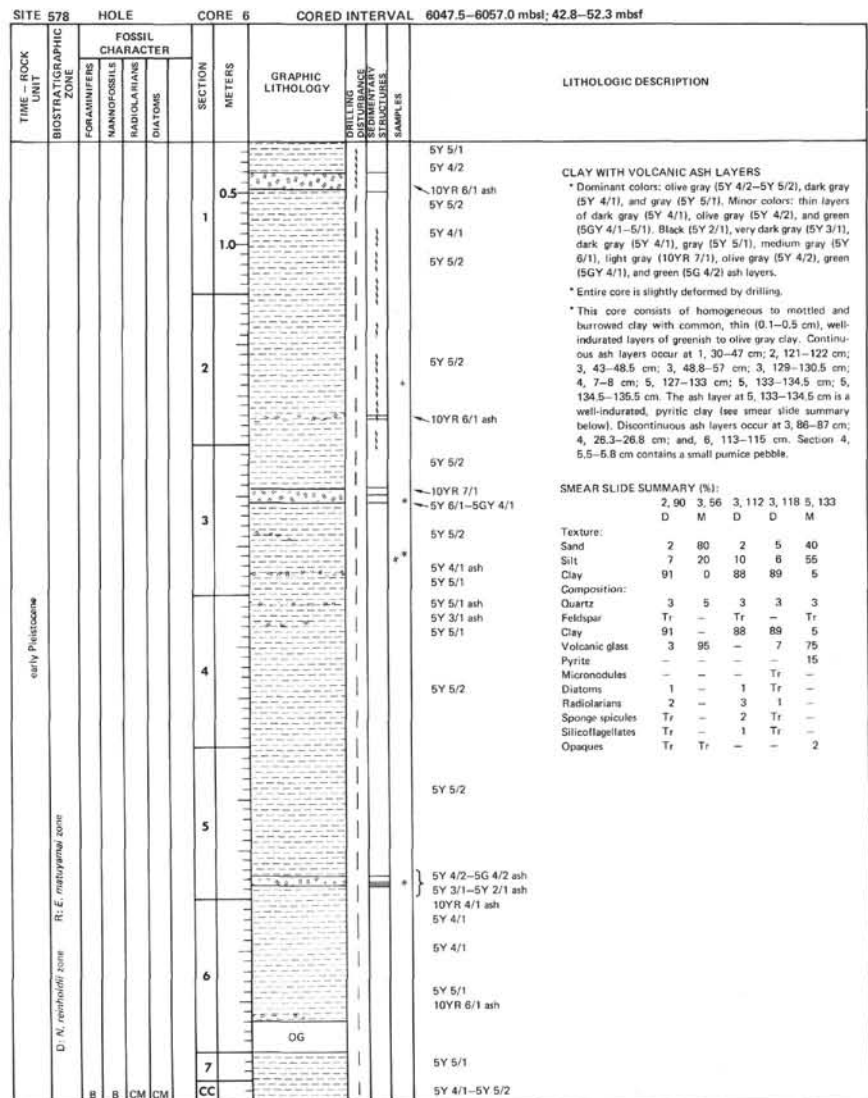
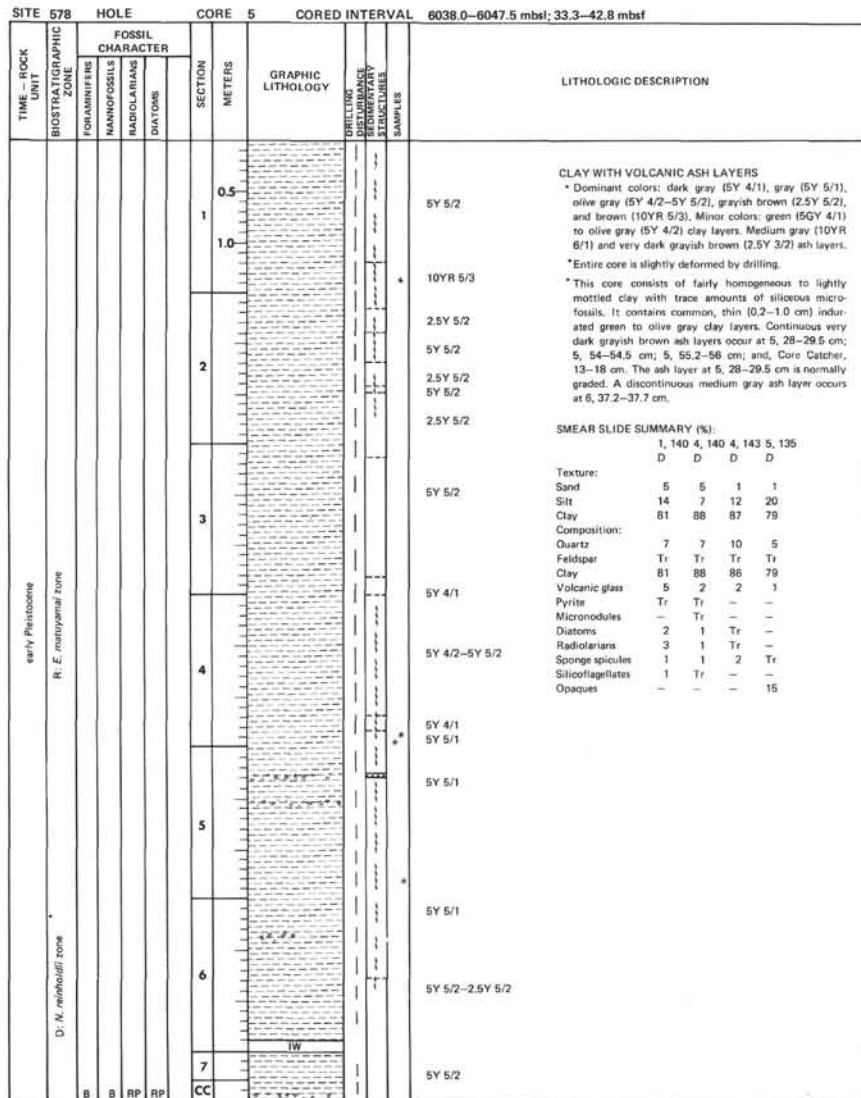
Overall, Site 578 was highly successful. The excellent quality of the cores and virtually full recovery, as well as the rapid sedimentation rate during the past 5 m.y., provide excellent records of ash deposition and magnetic reversals during this period. This site also fixes the onset of biosiliceous sedimentation at the southern limit of the north-south transect from Sites 578 to 581. The deeper pelagic clay section complements those at Site 576 and LL44-GPC3, and provides the basis for an east-west profile of Paleogene authigenic sedimentation.

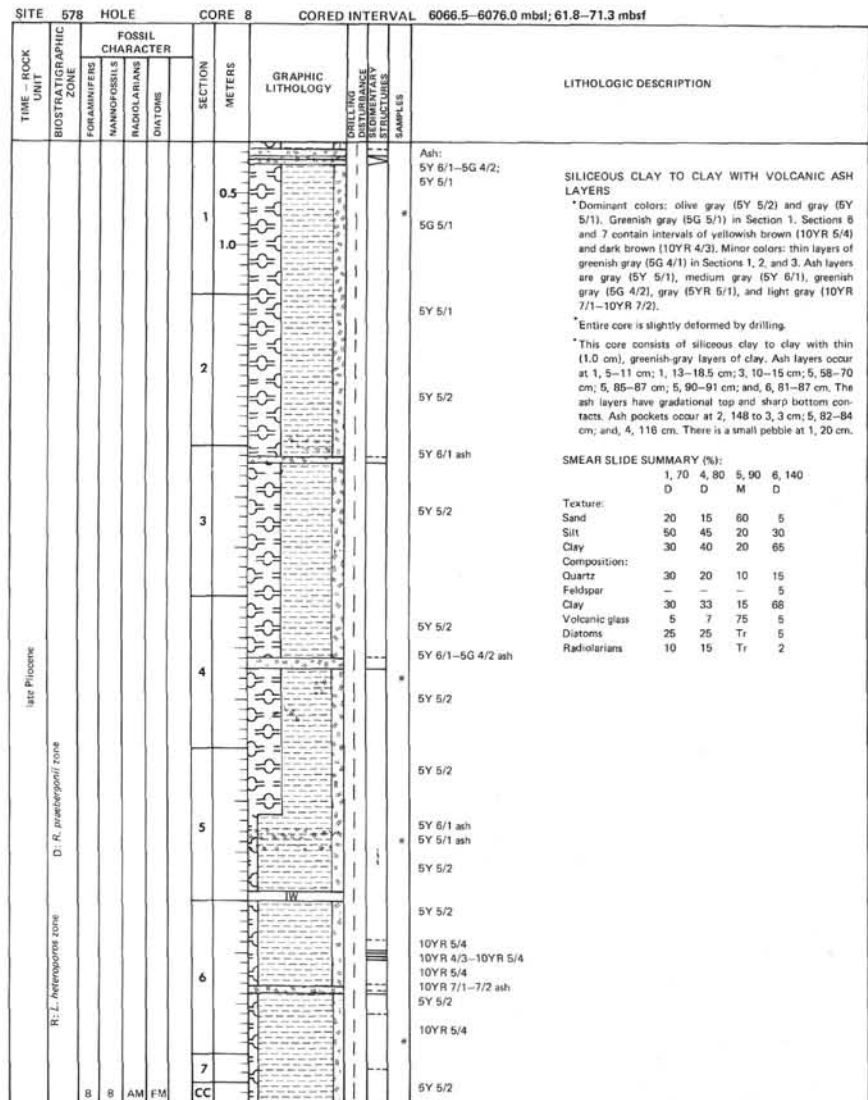
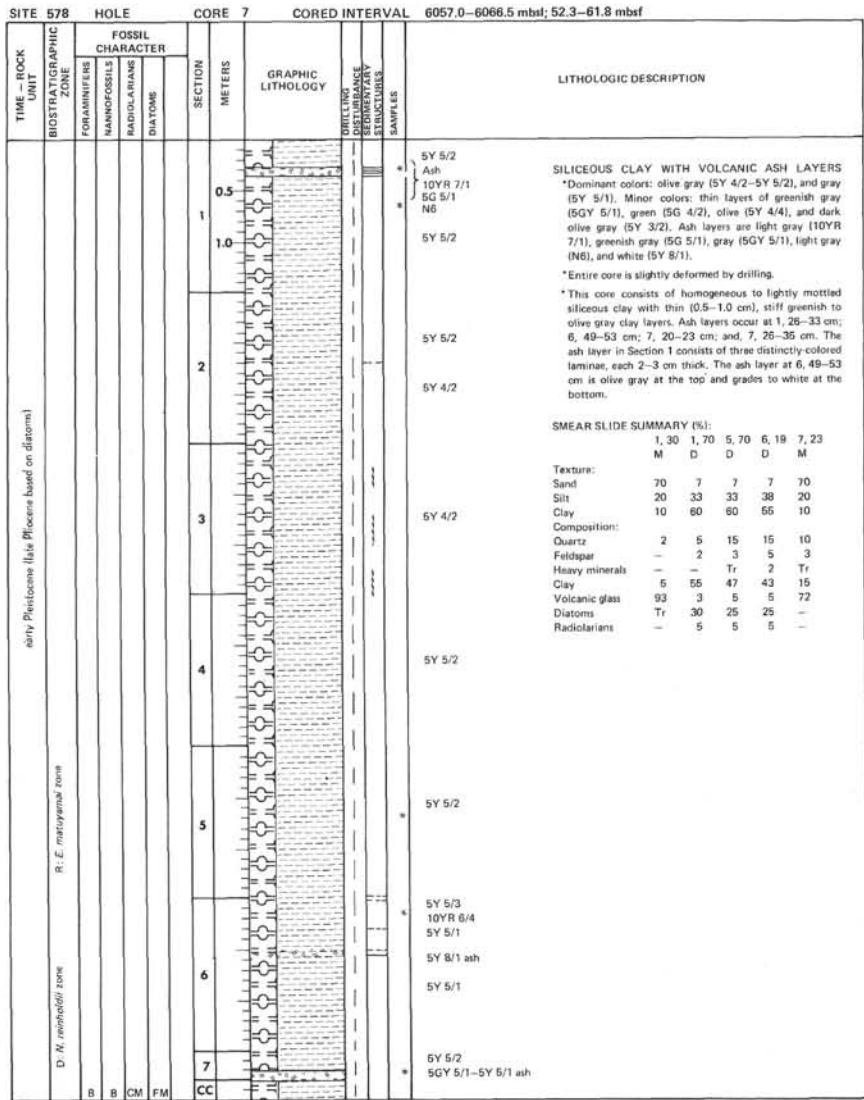
REFERENCES

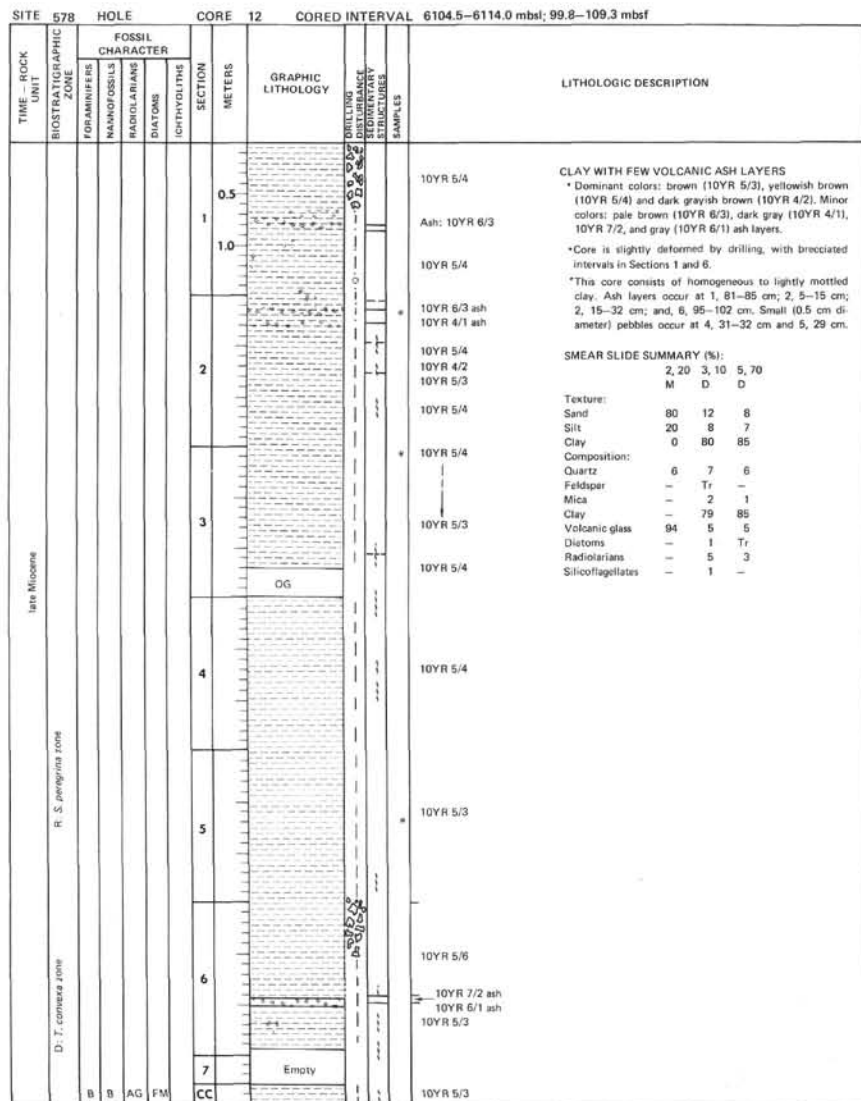
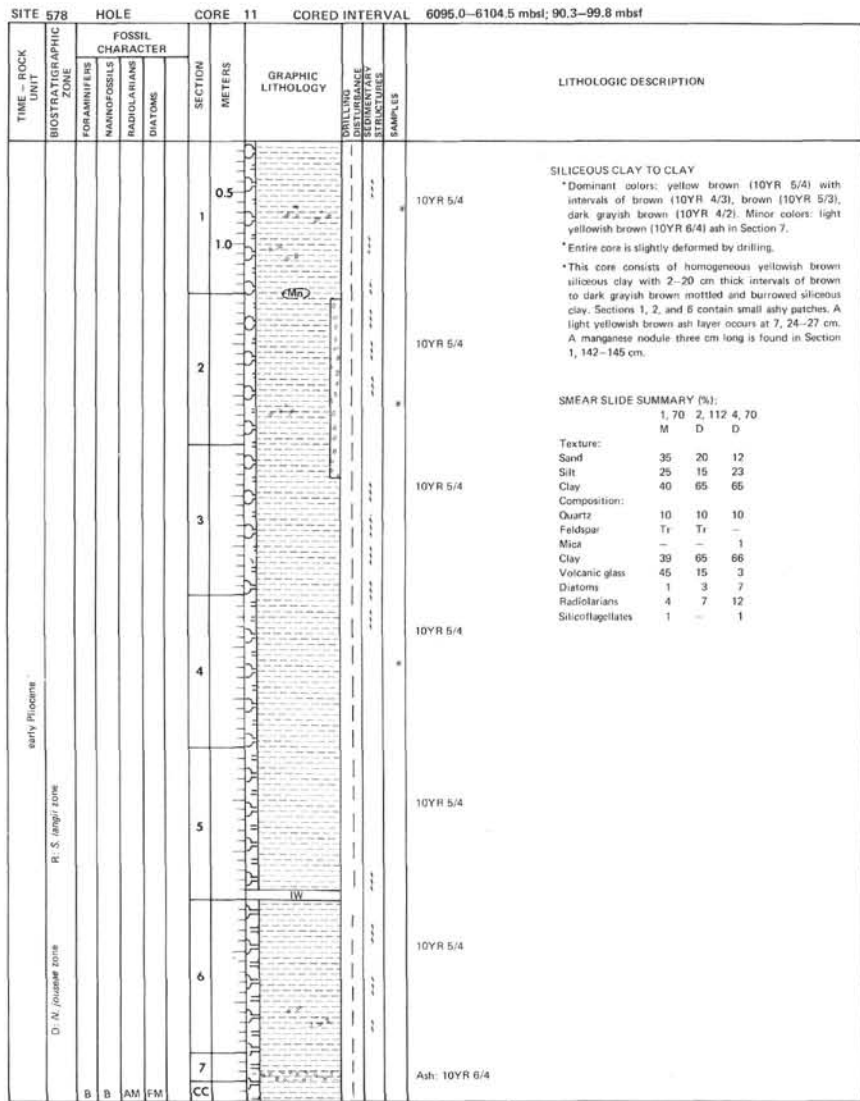
- Berggren, W. A., Kent, D. V., and Flynn, J. J., in press. Paleogene geochronology and chronostratigraphy. In Snelling, N. J. (Ed.), *Geochronology and the Geological Record*. Geol. Soc. London Spec. Pap.
- Blow, W. H., 1969. Late middle Eocene to Recent planktonic foraminiferal biostratigraphy. In Bronnimann, P. and Renz, H. H. (Eds.), *Proc. First Int'l. Conf. Planktonic Microfossils* (Vol. 6): Leiden (Brill), 199-421.
- Boyce, R. E., 1976a. Definitions and laboratory techniques of compressional and sound velocity parameters and wet-water content, wet-bulk density, and porosity parameters by gravimetric and gamma ray attenuation techniques. In Schlanger, S. D., Jackson, E. D., et al., *Init. Repts. DSDP*, 33: Washington (U.S. Govt. Printing Office), 931-958.
- , 1976b. Deep Sea Drilling Project procedures for shear strength measurements of clayey sediment using modified Wykeham Farrance Laboratory Vane Apparatus. In Barker, P., Dalziel, I. W. D., et al., *Init. Repts. DSDP*, 36: Washington (U.S. Govt. Printing Office), 1059-1068.
- Burckle, L. H., Hammond, S. R., and Seyb, S. M., 1978. A stratigraphically important new diatom from the Pleistocene of the North Pacific. *Pac. Sci.*, 32(2):209-214.
- Damuth, J. E., Jacobi, R. D., and Hayes, D. E., 1983. Sedimentation processes in the northwest Pacific Basin revealed by echo character mapping studies. *Geol. Soc. Am. Bull.*, 94:381-395.
- Fischer, A. G., Heezen, B. C., et al., 1971. Site 47, In Fischer, A. G., Heezen, B. C., et al., *Init. Repts. DSDP*, 6: Washington (U.S. Govt. Printing Office), 67-144.
- Foreman, H. P., 1975. Radiolaria from the North Pacific, Deep Sea Drilling Project, Leg 32. In Larson, R. L., Moberly, R., et al., *Init. Repts. DSDP*, 32: Washington (U.S. Govt. Printing Office), 579-701.
- Hays, J. D., 1970. Stratigraphy and evolutionary trends of Radiolaria in North Pacific deep-sea sediments. In Hays, J. D. (Ed.), *Geological Investigations of the North Pacific*. Mem. Geol. Soc. Am., 126:185-218.
- Koizumi, I., 1973. The late Cenozoic diatoms of Sites 183-193, Leg 19, Deep Sea Drilling Project. In Creager, J. S., Scholl, D. W., et al., *Init. Repts. DSDP*, 19: Washington (U.S. Govt. Printing Office), 805-855.
- McDougall, I., 1977. The present status of the geomagnetic polarity time scale. Research School of Earth Sciences. *A.N.U. Publ.*, No. 1288.
- Ness, G., Levi, S., and Couch, R., 1980. Marine magnetic anomaly time scales for the Cenozoic and Late Cretaceous: a precis, critique, and synthesis. *Rev. Geophys. Space Phys.*, 18:753-770.
- Olsson, R. K., 1964. Late Cretaceous planktonic foraminifera from New Jersey and Delaware. *Micropaleontology*, 10(2):157-188.
- Pessagno, E. A., 1967. Upper Cretaceous planktonic foraminifera from the western Gulf Coastal Plain. *Paleontographica Americana*, 5(37):245-444.
- Postuma, J. A., 1971. *Manual of Planktonic Foraminifera*: Amsterdam (Elsevier).
- Riedel, W. R., and Sanfilippo, A., 1970. Radiolaria, Leg 4, Deep Sea Drilling Project. In Bader, R. G., Gerard, R. D., et al., *Init. Repts. DSDP*, 4: Washington (U.S. Govt. Printing Office), 503-575.
- Stainforth, R. M., et al., 1975. Cenozoic planktonic foraminiferal zonation and characteristics of index forms. *Univ. Kans. Paleontol. Contrib. Pap.*, 62:1-425.











SITE 578		HOLE		CORE 15		CORED INTERVAL		6133.0-6142.5 mbsl; 128.3-137.8 mbsf		
TIME - ROCK UNIT	BIOSTRATIGRAPHIC ZONE	FOSSIL CHARACTER				SECTION METERS	GRAPHIC LITHOLOGY	DRILLING DISTURBANCE STRUCTURES	SAMPLES	LITHOLOGIC DESCRIPTION
		FORAMINIFERS	MAMMOFOSILS	RADIOLARIANS	DIATOMS					
Miocene	B B B B					0.5				10YR 3/3
						1				10YR 3/3
						1.0				10YR 3/3
						2				10YR 3/3
						3				10YR 3/3
						4				10YR 3/3
						5				10YR 3/3
						6				10YR 3/3 10YR 4/3 10YR 3/3 10YR 4/3 10YR 3/3 10YR 4/3
						7				10YR 4/3 10YR 3/3 10YR 3/3
						CC				

PELAGIC CLAY
 * Dominant colors: dark brown (10YR 3/3) and brown (10YR 4/3) to dark brown (7.5YR 5/4) layer. Mottles in the core are yellowish brown (10YR 5/6) in Sections 1, 5, 6, and 7; brown (7.5YR 5/4) in Sections 2 and 3; and, reddish yellow (7.5YR 6/8) in Section 4.
 * Entire core is slightly deformed by drilling.
 * This core consists of pelagic clay with tiny, faint black mottles and larger reddish yellow to yellowish brown to brown mottles.

SMEAR SLIDE SUMMARY (%):

	2, 90		6, 60	
	D	D	D	D
Texture:				
Sand	0	0		
Silt	15	10		
Clay	85	90		
Composition:				
Quartz	7	5		
Feldspar	2	1		
Heavy minerals	3	-		
Clay	84	88		
Volcanic glass	3	2		
Palagonite	1	-		
Opacues	-	4		

10YR 5/3-5/4
 10YR 4/3
 7.5YR 5/4
 10YR 4/3

OG

SITE 578		HOLE		CORE 16		CORED INTERVAL		6142.5-6152.0 mbsl; 137.8-147.3 mbsf		
TIME - ROCK UNIT	BIOSTRATIGRAPHIC ZONE	FOSSIL CHARACTER				SECTION METERS	GRAPHIC LITHOLOGY	DRILLING DISTURBANCE STRUCTURES	SAMPLES	LITHOLOGIC DESCRIPTION
		FORAMINIFERS	MAMMOFOSILS	RADIOLARIANS	DIATOMS					
(middle) Miocene	B RP B B					0.5				10YR 4/3
						1				10YR 4/3
						1.0				10YR 4/3
						2				10YR 4/3
						3				10YR 3/3
						4				10YR 3/3
						5				10YR 3/3 10YR 3/2
						6				10YR 3/3 10YR 3/2 10YR 4/3 layer
						7				10YR 3/2
						CC				

PELAGIC CLAY
 * Dominant colors: Section 1 to Section 2, 64 cm is brown (10YR 4/3) to dark brown with brown (7.5YR 5/4) to brown (10YR 5/3) mottles. Section 2, 64 cm to Section 5, 125 cm is dark brown (10YR 3/3) with brown (10YR 5/3) and yellowish brown (10YR 5/4) mottles. Section 5, 125 cm to the Core Catcher is very dark grayish brown (10YR 3/2). Faint black mottles are present throughout the core.
 * Core is slightly deformed by drilling.
 * This core consists of lightly mottled pelagic clay.

SMEAR SLIDE SUMMARY (%):

	5, 7		5, 96		CC
	D	D	D	D	
Texture:					
Sand	2	1	5		
Silt	5	7	1		
Clay	93	92	94		
Composition:					
Quartz	2	5	5		
Feldspar	1	-	-		
Mica	Tr	2	-		
Clay	93	92	94		
Volcanic glass	Tr	1	Tr		
Palagonite	-	-	-		
Micronodules	-	-	1		
Opacues	5	-	-		

10YR 3/3 layer
 10YR 3/2
 10YR 4/3 layer

Empty

